



**HAL**  
open science

## **Functional benefit of structural disorder for the replication of measles, Nipah and Hendra viruses**

Frank Gondelaud, Giulia Pesce, Juliet F. Nilsson, Christophe Bignon, Denis Ptchelkine, Denis Gerlier, Cyrille Mathieu, Sonia Longhi

### ► **To cite this version:**

Frank Gondelaud, Giulia Pesce, Juliet F. Nilsson, Christophe Bignon, Denis Ptchelkine, et al.. Functional benefit of structural disorder for the replication of measles, Nipah and Hendra viruses. *Essays in Biochemistry*, 2022, 66 (7), pp.915-934. <10.1042/EBC20220045>. <hal-03794799>

**HAL Id: hal-03794799**

**<https://hal.science/hal-03794799v1>**

Submitted on 9 Oct 2023

**HAL** is a multi-disciplinary open access archive for the deposit and dissemination of scientific research documents, whether they are published or not. The documents may come from teaching and research institutions in France or abroad, or from public or private research centers.

L'archive ouverte pluridisciplinaire **HAL**, est destinée au dépôt et à la diffusion de documents scientifiques de niveau recherche, publiés ou non, émanant des établissements d'enseignement et de recherche français ou étrangers, des laboratoires publics ou privés.



HAL Authorization

# Functional Benefit of Structural Disorder for the Replication of Measles, Nipah and Hendra Viruses

Frank Gondelaud<sup>1</sup>, Giulia Pesce<sup>1</sup>, Juliet F. Nilsson<sup>1</sup>, Christophe Bignon<sup>1</sup>, Denis Ptchelkine<sup>1</sup>, Denis Gerlier<sup>2</sup>, Cyrille Mathieu<sup>2</sup> and Sonia Longhi<sup>1\*</sup>

<sup>1</sup> Lab. Architecture et Fonction des Macromolécules Biologiques (AFMB), UMR 7257, Aix-Marseille University and Centre National de la Recherche Scientifique (CNRS), Marseille, France

<sup>2</sup> NeuroInvasion, TROPism and VIRal Encephalitis (NITROVIRE), Centre International de Recherche en Infectiologie (CIRI), Université de Lyon, INSERM, U1111, CNRS, UMR 5308, Université Claude Bernard Lyon 1, Ecole Normale Supérieure de Lyon, Lyon, France

\* Correspondence: [Sonia.longhi@univ-amu.fr](mailto:Sonia.longhi@univ-amu.fr)

## Abstract

Measles, Nipah and Hendra viruses are severe human pathogens within the *Paramyxoviridae* family. Their non-segmented, single-stranded, negative-sense RNA genome is encapsidated by the nucleoprotein (N) within a helical nucleocapsid that is the substrate used by the viral RNA-dependent-RNA-polymerase (RpRd) for transcription and replication. The RpRd is a complex made of the large protein (L) and of the phosphoprotein (P), the latter serving as an obligate polymerase cofactor and as a chaperon for N. Both the N and P proteins are enriched in intrinsically disordered regions (IDRs), *i.e.* regions devoid of stable secondary and tertiary structure. N possesses a C-terminal IDR (N<sub>TAIL</sub>), while P consists of a large, intrinsically disordered N-terminal domain (NTD) and a C-terminal domain (CTD) encompassing alternating disordered and ordered regions. The V and W proteins, two non-structural proteins that are encoded by the P gene *via* a mechanism of co-transcriptional edition of the P mRNA, are prevalently disordered too, sharing with P the disordered NTD. They are key players in the evasion of the host antiviral response and were shown to phase separate and to form amyloid-like fibrils *in vitro*. In this review, we summarize the available information on IDRs within the N, P, V and W proteins from these three model paramyxoviruses and describe their molecular partnership. We discuss the functional benefit of disorder to virus replication in light of the critical role of IDRs in affording promiscuity, multifunctionality, fine regulation of interaction strength, scaffolding functions and in promoting liquid-liquid phase separation and fibrillation.

discuss the functional advantage of structural disorder for viral replication.

## Highlights

- Intrinsic disorder is a widespread property in the replicative complex of these three model paramyxoviruses
- Intrinsic disorder affords a way to finely tune the affinity of interactions critical for viral transcription and replication
- Intrinsic disorder confers promiscuity and multifunctionality
- Intrinsic disorder promotes liquid-liquid phase separation, phase transition and fibrillation
- Intrinsic disorder enables lessening evolutionary constraints

## Introduction

The measles virus (MeV), together with the cognate Nipah and Hendra viruses (NiV and HeV, *Henipavirus* genus) are severe human pathogens belonging to the *Paramyxoviridae* family within the *Mononegavirales* order. Paramyxoviruses are enveloped viruses with a non-segmented, single-stranded RNA genome of negative polarity. Their envelope is composed of a lipid bilayer, derived from the host cell plasma membrane, into which are inserted the F and G glycoproteins. The matrix protein (M) forms a layer beneath the envelope bridging the cytoplasmic tails of the glycoproteins with the nucleocapsid (NC) (**Fig. 1A**).

The genome of paramyxoviruses is encapsidated by the nucleoprotein (N) within a helical NC [1,2]. The NC, and not naked RNA, is the template used by the RNA-dependent RNA polymerase (RdRp) during transcription and replication. The RdRp is a complex made of the large (L) protein, which bears all the enzymatic activities, and the phosphoprotein (P). Cryo-electron microscopy (EM) structures of L proteins from various *Mononegavirales* members unveiled a conserved structural organization consisting in five globular domains connected by flexible linkers (for reviews see [3,4]). The ribonucleoprotein (RNP) complex, made of encapsidated RNA, P and L, constitutes the replicative complex and the minimal infectious unit (**Fig. 1A**). Transcription and replication take place in so-called “viral factories”, *i.e.* cytoplasmic inclusions (referred to as inclusions bodies, IBs) that serve as platforms for optimized viral replication, thanks to selective uptake or exclusion of components and shielding from the host innate immune defense.

The P protein is an essential polymerase cofactor: (i) it keeps L in a soluble and active form [5-7], (ii) it allows L recruitment onto the nucleocapsid template [7] and (iii) it regulates viral RNA synthesis [8] (**Fig. 1A**). P also serves as a chaperon for N: by forming a soluble complex with monomeric N (N<sup>o</sup>) [9,10] it prevents the self-assembly of N on cellular RNA in the absence of ongoing viral genomic RNA synthesis [11,12] (for reviews see [13-20]).

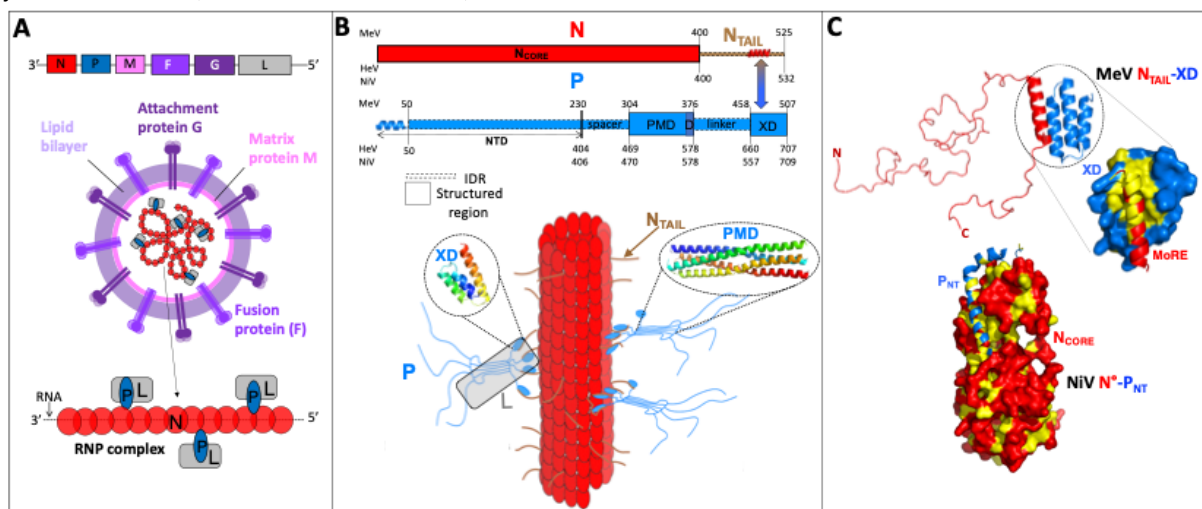


**Figure 1. Scheme of the organization of paramyxoviral genome and particle, of the N and P proteins and structure of the N<sub>TAIL</sub>-XD and N<sup>o</sup>-P<sub>NT</sub> complexes. (A)** Schematic representation of paramyxoviral genome and particle. The negative-sense genomic RNA is presented in the 3' to 5' orientation. **(B)** Top: modular organization of N and P proteins from MeV, NiV and HeV. Structured and disordered regions are represented as large or narrow boxes respectively. N<sub>CORE</sub>: N structured region; N<sub>TAIL</sub>: intrinsically C-terminal region of N. NTD: N-terminal region of P; PMD: P multimerization domain; XD: X domain of P; D, dynamic region conditionally disordered in MeV PMD (aa 358-375 of P). The  $\alpha$ -MoREs at the N-terminal region of P and within N<sub>TAIL</sub>, partly preconfigured in solution and adopting a stable  $\alpha$ -helical conformation upon binding to N<sup>o</sup> and XD, respectively, are shown as helices. Bottom: schematic representation of the nucleocapsid (NC) with N<sub>TAIL</sub> exposed at its surface. P is shown as a tetramer attached to the NC via XD. The structures of MeV XD (PDB code 1OKS) [21] and of PMD (PDB code

4BHV [22]) are shown. XD is shown in rainbow with blue corresponding to the N-terminus and red to the C-terminus. (C) Top: cartoon representation of the MeV N<sub>TAIL</sub>-XD complex (PDB code 1T6O) [23] in which the fuzzy N- and C-terminal appendages were drawn at scale by extracting the corresponding regions from a representative member of the MeV N<sub>TAIL</sub> conformational ensemble deposited in the Protein Ensemble Database (PED) [24] (PED entry code 00020). The structure of XD (aa 459-507 of P) bound to the MoRE of N<sub>TAIL</sub> (aa 486-504 of N) is also shown with XD in surface representation and the MoRE in ribbon. Hydrophobic residues are shown in yellow. Bottom: Structure of the NiV N<sup>o</sup>-P<sub>NT</sub> complex (PDB code 4CO6) [9] with the same color code as in the top panel. All structures were drawn using Pymol [25].

### *Order and disorder within the N and P proteins*

The N and P proteins from MeV, NiV and HeV possess long intrinsically disordered regions (IDRs), *i.e.* functional regions devoid of stable secondary and tertiary structure [26]. The N protein consists of two domains: a structured N-terminal domain (N<sub>CORE</sub>), responsible for RNA binding and for self-assembly, and a C-terminal IDR (N<sub>TAIL</sub>) that binds to the C-terminal region of P [27-30] (**Fig. 1B**) and that is also disordered in the context of the nucleocapsid [31-33]. The structure of N either in its monomeric form bound to P (N<sup>o</sup>-P) or in its self-assembled state has been solved in a number of paramyxoviruses and of closely related pneumoviruses (for a review see [20]).

The P protein consists of a long N-terminal intrinsically disordered domain (NTD) and a C-terminal region that has a modular organization being composed of alternating disordered and structured regions (**Fig. 1B**) [29,34-37]. At the N-terminus of P there is a short order-prone molecular recognition element ( $\alpha$ -MoRE) that undergoes  $\alpha$ -helical folding upon binding to N<sup>o</sup> (**Fig. 1C**) and whose location at the surface of N<sup>o</sup> prevent its self-assembly into NC [19,20]. An additional short order-prone region establishing weak interactions with N<sup>o</sup> was identified within the NTD and shown to be crucial for MeV transcription and replication [38].

The P structured regions are the P multimerization domain (PMD), responsible for P oligomerization, and the X domain (XD) that is responsible for N<sub>TAIL</sub>-mediated attachment of P to the NC and for binding to L [7,39]. Although the N<sub>TAIL</sub>- and L-binding sites are located in two distinct XD regions, binding of N<sub>TAIL</sub> to XD prevents XD from recruiting L [39]. While PMD consists in a coiled-coil [22,36,40-43] XD adopts a triple  $\alpha$ -helical bundle conformation [21,30,32] (**Fig. 1B**).

Interestingly, the folded regions of P exhibit some degree of conformational heterogeneity and residual disorder. Native mass spectrometry studies indicated that MeV XD populates at least two conformations under native conditions [44], and equilibrium and kinetic measurements, combined with molecular dynamic simulations, unveiled the presence of a folding intermediate [45] (**Fig. 2A**). Likewise, NiV XD was found to adopt a two-helix conformation in crystals (**Fig. 2B**), and to fold into the canonical triple helical bundle upon binding to the MoRE of N<sub>TAIL</sub> [46]. In solution, both NiV XD and HeV XD are in conformational equilibrium between the canonical three-helix bundle and a less populated elongated two-helix hairpin, although only NiV XD is able to dimerize [46]. A recombinant NiV encoding a chimeric P bearing HeV XD is attenuated [46], advocating for a scenario where XD stability and conformational diversity could be exploited by the virus to regulate P binding to the NC and/or to L. In further support of a conformational heterogeneity of XD, X domains of rubulaviruses (another genus of the *Paramyxoviridae* family) span a structural continuum ranging from stable or transiently populated  $\alpha$ -helical bundles, to largely disordered conformations in solution [47,48].

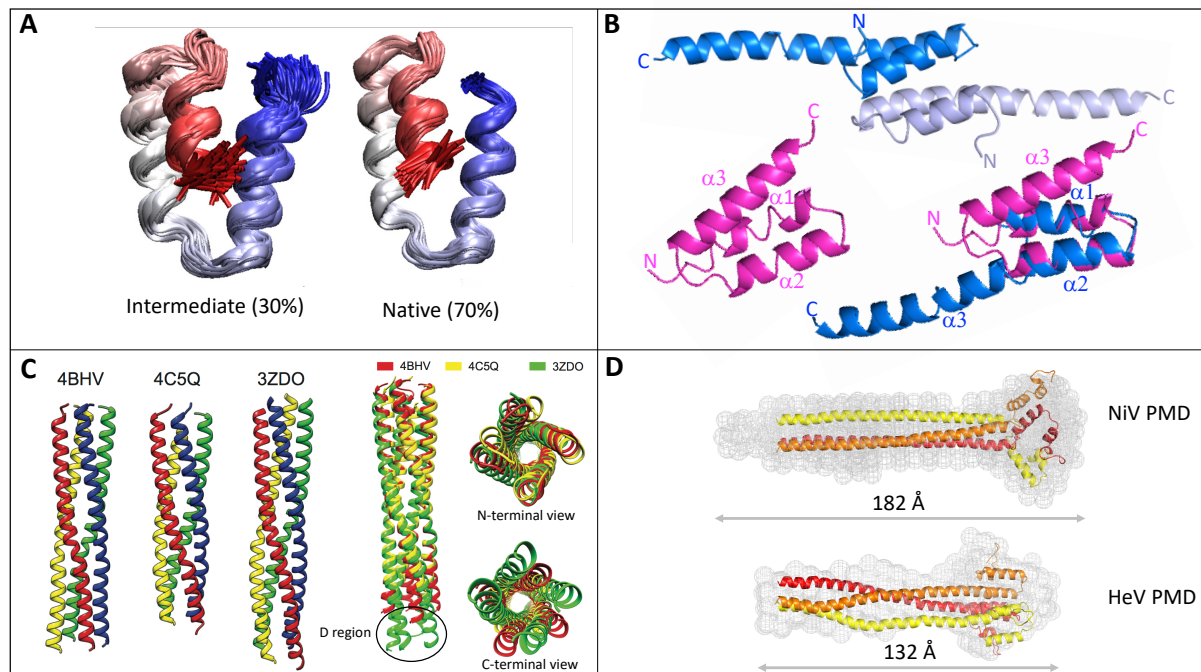


**Figure 2. Structures of XD and PMD.** (A) Replica-averaged meta-dynamic ensemble of MeV XD highlighting the presence of a native state and of an intermediate state populated at 70% and 30%, respectively [45]. (B) Ribbon representation of the dimeric two-helix conformation of NiV XD as observed in crystals (PDB code 7PON) [46] (top panel), and of HeV XD (pink) (PDB code 4HEO) [32] either alone (left bottom panel) or superposed to a monomer of NiV XD (right bottom panel). (C) Structural comparison of MeV PMD structures. Left: ribbon representations of the crystal structures of the MeV PMD tetramers as observed in the three different MeV PMD forms solved to date. Right: superimposition of the three MeV PMD tetramers, with PDB codes 4BHV, 4C5Q, [22] and 3ZDO [41] shown in red, yellow, and green, respectively. The conditionally disordered “dynamic” C-terminal region of PMD (D) is circled. Data are from [22] and reproduced with permission of the International Union of Crystallography (<http://journals.iucr.org/>). (D) Structural models of the trimeric coiled-coil PMDs of NiV [42] and HeV [43] embedded into their SAXS-derived *ab initio* envelopes. All structures were drawn using Pymol [25].

In the same vein, structural comparison among available crystal structures of MeV PMD unveiled not only unexpected and significant differences in the quaternary structure of the tetrameric coiled-coil, but also in the extent of disorder in its C-terminal region [22] (**Fig. 2C**). If previous data showed that the L-P interaction requires the C-terminal region of PMD, the “linker” region and XD [5,39], the C-terminal conditionally disordered region (referred to as “dynamic” region, D) was found to be critical for maturation of L, *i.e.* for maintaining it in a soluble form [7].

Likewise, the cohesiveness of the coiled-coil has a profound impact on transcription and replication: stabilizing or destabilizing PMD dramatically affects P function, where P works within a narrow window of stability and its sequence is naturally optimized for transcription and replication [7] (**Fig. 3A**). Therefore, residual disorder within PMD and variations in cohesiveness of the coiled-coil are critical for interaction with L and for transcription and replication.

*Henipavirus* PMDs exhibit an even more pronounced conformational heterogeneity, where NiV PMD was found to form tetramers in crystals [36,40] and trimers in solution [42]. SAXS studies revealed that HeV PMD is a trimer in solution too [43], although its N-terminal helical region has a different orientation with respect to that of NiV PMD in solution (**Fig. 2D**) [43]. In light of the high sequence similarity between NiV and HeV PMDs, these structural differences likely reflect an intrinsic ability of *Henipavirus* PMDs to undergo conformational changes resulting in forms of different lengths and compaction, although the triggering factors remain elusive. By analogy with MeV PMD [7], it is tempting to speculate that these different forms could regulate binding to L and hence ultimately

transcription and replication.

### *The N<sub>TAIL</sub>-XD interaction: molecular mechanisms, fuzziness and functional impact*

In the three viruses N<sub>TAIL</sub> binds to XD (**Fig. 1B, 1C**) with a 1:1 stoichiometry and with an equilibrium dissociation constant (K<sub>D</sub>) in the  $\mu\text{M}$  range [30,49,50]. Interaction with XD triggers  $\alpha$ -helical induced folding within an  $\alpha$ -MoRE of N<sub>TAIL</sub> [27,28,30-33,49,51-55]. In its free form, the MoRE is partly preconfigured as an  $\alpha$ -helix [31-33] yet it folds according to a folding after binding mechanism [32,50,56,57]. In the bound form, the MoRE is embedded between helices  $\alpha_2$  and  $\alpha_3$  of XD to yield a pseudo-four helix arrangement mainly stabilized by hydrophobic contacts (**Fig. 1C**) [21,23,27,30,32]. Electrostatic interactions play an additional role in properly orienting the *Henipavirus* MoRE at the XD surface [32,58].

The MeV N<sub>TAIL</sub>-XD complex is “fuzzy” [59], *i.e.* it retains a considerable amount of residual disorder, with the regions preceding and following the MoRE being embedded in a long [60] and short [61] fuzzy appendage, respectively (**Fig. 1C**). The fuzziness of the *Henipavirus* N<sub>TAIL</sub>-XD complex is even more pronounced, with the MoRE undergoing helical fraying at the surface of XD [32,33]. The long, N-terminal fuzzy appendage was found to act as a natural dampener of the N<sub>TAIL</sub>-XD interaction and to slow down the rate of folding of the MoRE [62] through a combination of entropic and enthalpic effects [63]. Increasing the  $\alpha$ -helical content of the MoRE results in increased interaction strength towards XD and higher folding rates [64] likely through a reduction of the entropic penalty. Conversely, decreasing its helicity has the opposite effect [64].

According to the so-called cartwheeling mechanism, which posits that the polymerase complex cartwheels from one N monomer to another within the NC [65], the N<sub>TAIL</sub>-XD interaction has to be dynamically established and broken to ensure progression of the L-P complex onto the NC to allow transcription and replication. If a too weak interaction would result in detachment of the L-P complex from the NC, a too much strong interaction is predicted to hinder the polymerase processivity. In the course of evolution, the length of the fuzzy region preceding the MoRE has likely been under selective pressure so as to ensure a balanced affinity towards XD. In support of this scenario, shortening this region results in an unbalance between transcription and replication [66,67]. Mutational studies that targeted XD unveiled that an increase in the affinity of the N<sub>TAIL</sub>-XD pair is associated to a reduction in transcript accumulation rate [8], thus further underscoring the role of the N<sub>TAIL</sub>-XD interaction in tightly controlling the viral polymerase progression along the NC template. The corollary of this is that the N<sub>TAIL</sub>-XD interaction strength has to be kept into a precise window to ensure efficient transcription and replication. In line with this requirement, random mutagenesis studies showed that the MoRE is poorly evolvable in terms of its binding abilities towards XD, suggesting that the sequence of the MoRE has been naturally selected to optimally bind XD, hence explaining its conservation in naturally occurring MeV strains [68]. This finding mirrors the one pertaining PMD whose sequence appears to be naturally optimized to bind L [7].

Combined biophysical and virological approaches that made use of N<sub>TAIL</sub> variants bearing substitutions within the MoRE enabled deciphering the functional impact of the MeV N<sub>TAIL</sub>-XD interaction and unveiled that the affinity of the binding reaction dictates the efficiency of transcription re-initiation by the viral polymerase at each intergenic region (IGR) within the viral genome [69]. When the viral polymerase has finished transcribing the first gene, it has to recognize the IGR region as a “separator” signal and to start transcribing the downstream gene. At each IGR the polymerase has a certain probability to fail re-initiating transcription of the downstream gene, which gives rise to a characteristic gradient of relative abundance of each mRNA (**Fig. 3B**). Our mutational studies showed

that the efficiency with which the polymerase re-initiates transcription of the downstream gene depends on the affinity between  $N_{TAIL}$  and XD (**Fig. 3C**). The interaction between  $N_{TAIL}$  and XD is naturally optimized to allow the viral polymerase to synthesize each of the viral messengers in proportions ensuring a balanced production of each of the viral proteins. Overall, mutational and deletion studies support the conclusion that a disordered appendage length code and an amino acid code of  $N_{TAIL}$  have shaped the interaction between  $N_{TAIL}$  and XD during evolution to ensure a balanced affinity for efficient transcription and replication.

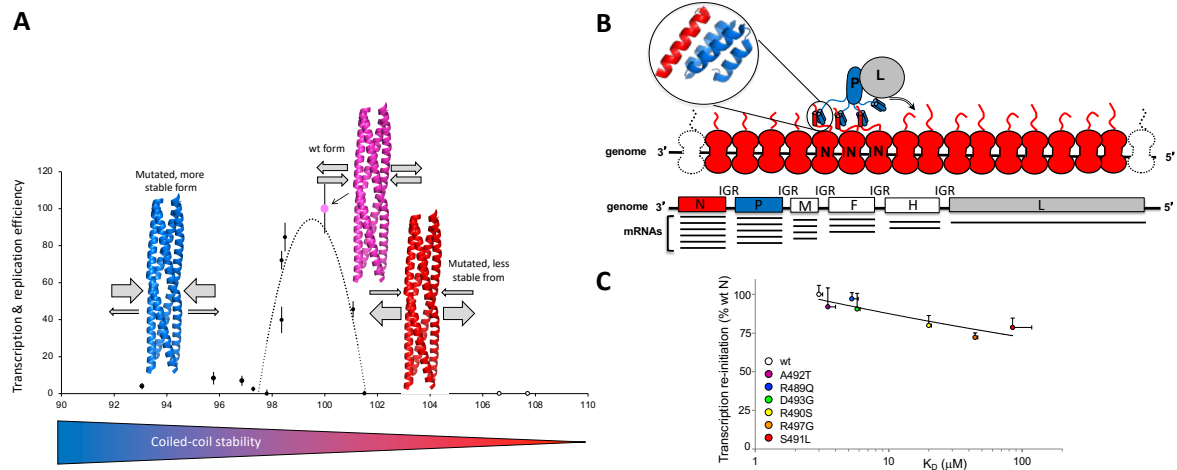


**Figure 3. Functional impact of variations in MeV PMD coiled-coil cohesiveness and  $N_{TAIL}$ -XD affinity.** (A) Relationship between MeV PMD coiled-coil stability and efficiency of transcription and replication, as determined in minireplicon studies [7]. The stability of the *wt* form (pink) is optimal for transcription and replication, whereas more stable (left, blue) or less stable (right, red) PMD forms are associated to a decreased efficiency. (B) Upper panel: Schematic representation of the movement of the L-P complex along the NC. Attachment of the L-P complex to the NC relies on the  $N_{TAIL}$ -XD interaction. Lower panel: schematic organization of the MeV genome with its 6 genes, separated by inter-gene regions (IGRs). Transcribed mRNAs are shown under each gene in their relative abundance. (C) Relationship between affinity of the  $N_{TAIL}$ -XD pair and efficiency with which the viral polymerase re-initiates transcription at the downstream gene. The transcription re-initiation efficiency of a set of single-site variants relative to the *wt* form, as observed in minireplicon studies with a dual-gene reporter system, are plotted as a function of the  $N_{TAIL}$ -XD affinity. Data were taken from [69]. All structures were drawn using Pymol [25].

### The V and W proteins, their functional role and their ability to phase separate and fibrillate

Like in many paramyxoviruses, including MeV [70], the P gene from HeV and NiV also encodes the C, V and W proteins. While the C protein is encoded in an alternative reading frame of the P gene, the V and W proteins result from the addition of either one (V) or two (W) non-templated guanosines at the editing site of the P mRNA (**Fig. 4A**). The latter is located at the end of the region encoding the NTD of P (**Fig. 4A**). Consequently, the P, V and W proteins share a common NTD but have distinct C-terminal domains (**Fig. 4A**).

The V and W proteins are key players in the evasion of the host innate immune response. [71-73]. They counteract the antiviral response by binding or hijacking key cellular proteins (**Fig. 4A**). They antagonize interferon (IFN) signaling by targeting STAT proteins that are key signal transducers of IFN-induced antiviral response [71]. V and W bind STAT1 through their NTD, with this ability being also conserved in NiV P [36]. V inhibits nuclear translocation of STAT1 and promotes its ubiquitination and degradation [74]. This latter property of V relies on its ability to bind to DDB1, a component of the ubiquitin ligase E3 complex, with the  $V_{CTD}$  playing a critical role in DDB1 recruitment [75]. The W protein sequesters STAT1 into the nucleus [76] thanks to a nuclear localization signal (NLS) that is recognized by importin  $\alpha$  [77] and accounts for steady-state location of the W protein in the nucleus

[78]. In addition to STAT1, the NiV P, V and W proteins, along with the HeV V and W proteins, also bind to STAT2 [79] and STAT4 [80], and NiV V also binds to STAT5 [80]. Beyond its antagonist activity of IFN signaling, NiV W also prevents IFN- $\beta$  expression and inhibits TLR3 signaling. In addition, V also prevents the detection of viral dsRNA by binding to MDA5, LGP2 [81], and PLK1 [82]. Finally, *Henipavirus* W proteins bind to 14-3-3 proteins, with this interaction resulting in modulation of various cellular processes including apoptosis [83] and inhibition of NF- $\kappa$ B-induced proinflammatory response [84].

The NTD of the NiV and HeV V proteins is disordered not only in isolation [29,36,37] but also in the context of the V protein, while the CTD adopts a zinc-finger conformation (**Fig. 4**) [75]. By contrast, the CTD of the W proteins is predicted to be disordered and the W proteins were shown to be intrinsically disordered (**Fig. 4A**) [85].

IDPs and/or IDRs are known for their involvement in a broad range of phase separation behaviors [86-88]. IDRs can drive liquid-liquid phase separation (LLPS), and the resulting biomolecular condensates can undergo “maturation” towards a gel or solid state that ultimately can nucleate amyloid-like fibrils [87,89-92]. *Vice versa*, amyloid-like fibers can form highly stable hydrogels [93,94]. Although gelation and fibrillation appear to be intertwined, they are not always interconnected: indeed, IDRs can form amyloid-like structures not only from hydrogels [95-97] but also from liquid samples [98-100].

In agreement with these properties, the HeV V protein jellifies *in vitro* (**Fig. 4B**). The minimal HeV V region responsible for this ability (referred to as PNT3, aa 200-310 of HeV V) is located within the intrinsically disordered NTD (**Fig. 4B**) [101,102]. Turbidity measurements showed that PNT3 phase separates and FRAP studies revealed a solid-like nature of the resulting condensates. Binding assays to the amyloid-specific dye Congo red, together with negative-staining transmission electron microscopy (TEM) studies, showed that PNT3 forms amyloid-like fibrils (**Fig. 4B**) [102]. Noteworthy, Congo red staining experiments provided hints that these amyloid-like fibrils form not only *in vitro* but also *in cellula* after transfection or infection of mammalian cells [102]. As predictable from the fact that the minimal amyloidogenic region (*i.e.* PNT3) is also present within the W protein, both NiV and HeV W proteins phase separate and form amyloid-like fibrils (**Fig. 4C**) [85]. Noteworthy, analysis of the Cryptic Amyloidogenic Regions Database (CARs DB, <http://carsdb.ppmclab.com/>) [103] revealed the presence of 6 CARs within the intrinsically disordered NTD of the HeV and NiV P proteins. Strikingly, one of these CARs (*i.e.* I<sub>208</sub>PEYYYG<sub>214</sub> in HeV and I<sub>208</sub>AEHYYG<sub>214</sub> in NiV) corresponds to an amyloidogenic region that we previously identified and experimentally validated within the NTD common to the HeV P, V and W proteins [102].

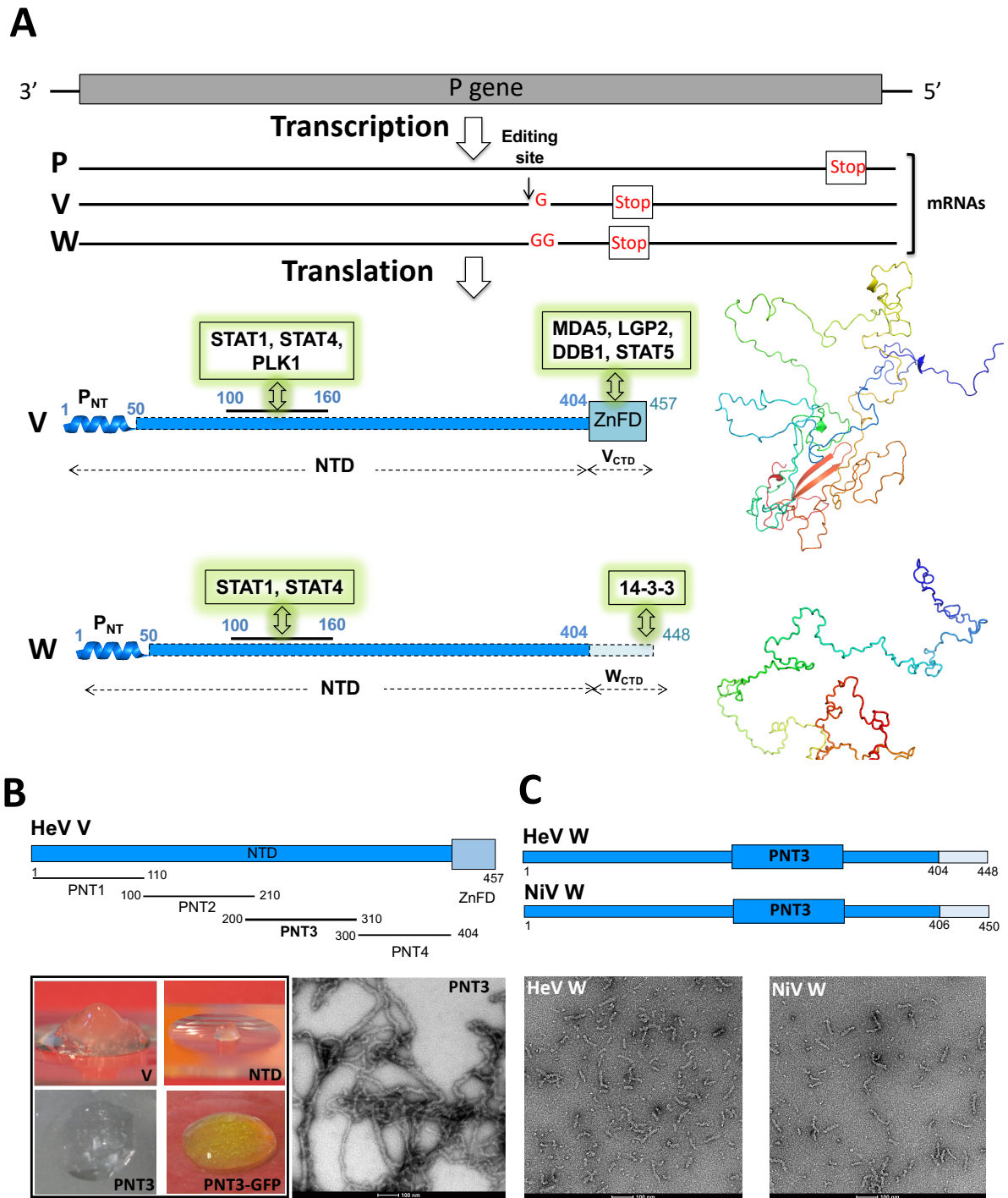


**Figure 4. Coding capacity of the P gene, structural organization of the *Henipavirus* V and W proteins and their ability to jellify and form amyloid-like fibrils. (A) Coding capacity of the P gene and modular organization of the *Henipavirus* V and W proteins. The C protein is not shown for the sake of clarity. Shown is the organization of HeV V and W proteins that is very close to that of their NiV counterpart. Structured and disordered regions are represented as large or narrow boxes respectively. NTD: N-terminal region common to the P, V and W proteins; ZnFD: zinc-finger domain; V<sub>CTD</sub> and W<sub>CTD</sub>: C-terminal domain of the V and W proteins; P<sub>NT</sub>:  $\alpha$ -MoRE adopting a stable  $\alpha$ -helical conformation upon binding of P to N<sup>o</sup> (*i.e.* N<sup>o</sup>-P<sub>NT</sub> complex) [9] or of V to host cellular transporters [104]. Well-described interaction sites with human cell partners involved in the innate immune response are shown. For both the V and W proteins, shown is a representative conformer, selected from the corresponding conformation ensemble (PED entry codes 00182 and 00204 for HeV V [102] and HeV W [85], respectively). (B) Hydrogels formed upon freezing and thawing of purified V, NTD, PNT3 and PNT3-GFP, and negative staining TEM micrograph of PNT3. Modified from [102]. (C) Negative staining TEM micrograph of the HeV and NiV W proteins. Modified from [85]. Structures were drawn using Pymol [25].**

### Functional benefits of disorder within N and P/V/W proteins

As described above, and reviewed in [19], compelling experimental evidence point to the abundance of structural disorder in the N and P/V/W proteins of paramyxoviruses. Which is the functional benefit that IDRs within the N and P/V/W proteins bring to these viruses that couldn't be afforded by structured counterparts? Below, we discuss the functional advantages of structural disorder.

#### Disorder as a determinant of nucleocapsid polymorphism

As mentioned above, N<sub>TAIL</sub> remains prevalently disordered in the context of the NC [31-33]. Its first 50 residues are however conformationally restrained being located in the interstitial space between successive turns of the NC [31,32] (Fig. 5A). The intrinsic flexibility of this region explains the increased rigidity of NCs in which N<sub>TAIL</sub> has been cleaved off (Fig. 5B, C) [28]. Its flexibility (and hence its potential to undergo conformational changes) is likely also responsible for the observed variations in pitch and twist in paramyxoviral NCs (Fig. 5D, left) [105-108]. In turn, these conformational differences may affect the recognition of the replication and transcription promoters (Fig. 5D). The replication promoter, located at the 3' end of the viral genome, consists of two discontinuous elements that form a functional unit when juxtaposed on two successive helical turns [109] (Fig. 5D). Thus, variations in the helical conformation of the NC, expectedly triggered by partner-induced N<sub>TAIL</sub> conformational changes, would result in a modification in the number of N monomers *per* turn, thereby ultimately governing the switch between transcription and replication *via* the disruption of the replication promoter at the expenses of the transcription promoter (or *vice versa*).

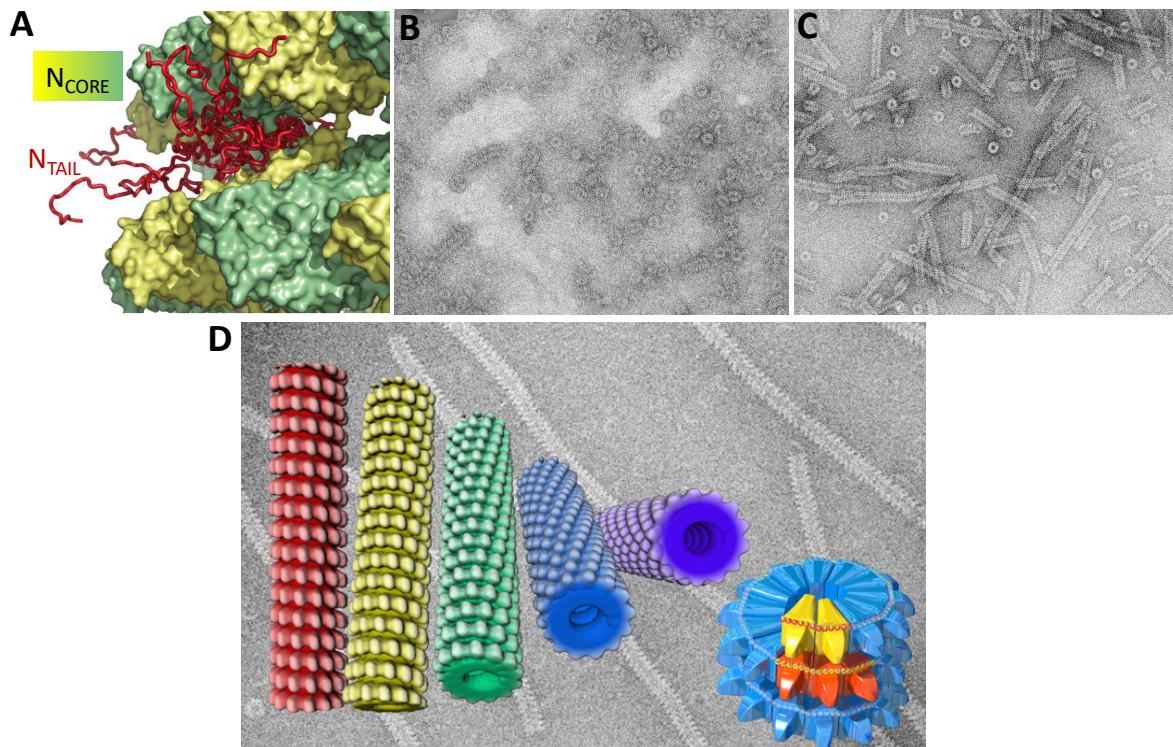


**Figure 5. Model of MeV nucleocapsid and illustration of the impact of N<sub>TAIL</sub> on the morphology of the nucleocapsid. (A)** Model of the MeV nucleocapsid. N<sub>CORE</sub> monomers are shown in yellow and green. The disordered N<sub>TAIL</sub> region is shown in red. Modified from [31]. **(B, C)** Negative staining electron microscopy pictures of MeV NC before **(B)** and after **(C)** incubation with trypsin. Modified from [28]. **(D)** Reconstruction by cryo-electron microscopy (left) [107,108] and schematic representation (right) of the MeV nucleocapsid. The bipartite

replication promoter is shown encapsidated by N monomers in yellow and red. Background: electron micrographs of MeV nucleocapsid (courtesy of D. Bhella, MRC, Glasgow, Scotland).

#### *Disorder as an exquisitely efficient solution for modulating binding affinities*

Two critical interactions for paramyxovirus transcription and replication, *i.e.* N<sup>0</sup>-P<sub>NT</sub> and N<sub>TAIL</sub>-XD, rely on a disordered segment that undergoes  $\alpha$ -helical folding upon binding to the structured partner. Why have these viruses conserved this peculiar interaction mode? Structural disorder is known to allow protein interactions to occur with both high specificity and low affinity [110-118]. The low affinity arises from the entropic penalty that is associated to the disorder-to-order transition. However, the persistence of residual disorder in IDP complexes (in the form of fuzzy appendages) together with the partial pre-configuration of binding motifs prior to binding, afford a way to modulate the binding affinity through variation of the entropic penalty (for a review see [119]). Static fuzziness, *i.e.* dynamic binding of the binding motif at the surface of the partner as in *Henipavirus* N<sub>TAIL</sub>-XD complexes, brings an additional means for regulating the interaction strength.

Because both the N<sup>0</sup>-P<sub>NT</sub> and N<sub>TAIL</sub>-XD interactions need to be continuously established and broken to ensure RNA synthesis, their interaction strength has to be tightly controlled. The involvement of IDRs in these complexes provides an exquisite means to modulate the interaction strength: by tuning the extent of pre-configuration of the binding motifs and/or the length of neighboring fuzzy appendages the virus can achieve an optimal binding strength. Besides, the extreme allostery that typifies IDPs (*i.e.* the long-range nature of the effects of substitutions), affords a supplementary layer of regulation. As a result, amino acid substitutions in fuzzy regions located far away from the binding site have the potential to affect binding [63,68].

Finally, conformational heterogeneity within PMD (*i.e.* differences in quaternary structure and cohesiveness, and ability to form different types of oligomers [22,42,43]), and within XD (*i.e.* ability to sample different conformations [44-46]), as well as residual disorder (*i.e.* “dynamic” region in PMD [22]) in P structured regions provide an additional way of regulating critical P-NC and/or P-L interactions [7,46], although the precise underlying molecular mechanisms remain to be elucidated.

#### *Disorder as a promoter of LLPS, phase transitions and fibrillation*

LLPS, a phenomenon that underlies the formation of membrane-less organelles (MLOs) and that has emerged as a novel mechanism of cell compartmentalization of biomolecules [98], is often driven by IDPs/IDRs either alone or in the presence of nucleic acids [86,120,121]. The phenomenon of LLPS is also exploited by viruses for their replication through the formation of condensates made of their own proteins either alone or in association with nucleic acids [122-127]. *Mononegavirales* members have broadly evolved mechanisms to assemble proteins into liquid-like viral factories [122,124,125,128,129]. Their liquid-like nature has been clearly demonstrated for MeV, where maturation of viral inclusions from a liquid-like to a gel-like state has been interpreted as a possible regulatory mechanism controlling organelle dynamics to optimize the viral replication cycle [130]. Co-expression of N and P proteins from a number of paramyxoviruses also leads to the appearance in transfected cells of spherical inclusions recapitulating the liquid properties of viral inclusions observed in infected cells. In all cases, the protein regions required for the formation of these inclusions are intrinsically disordered, thus illustrating the critical role of structural disorder in this functionally important process (for reviews see [122,125,128,131]). Purified MeV N and P proteins also phase separate *in vitro*, with PMD, the linker region and XD, together with full-length N in its monomeric form bound to P, being essential for LLPS (**Fig. 6A,B**) [132]. The combination of P<sub>1-50</sub>N<sub>1-525</sub> with P<sub>304-507</sub> is the minimal phase-separating system (**Fig. 6A,B**). RNA colocalizes within preformed droplets made of P<sub>1-50</sub>N<sub>1-525</sub> and P<sub>304-507</sub>, where it is readily

encapsidated within NC-like particles (Fig. 6C) [132]. Noteworthy, the encapsidation rate within droplets is enhanced compared to the dilute phase, providing strong indication that the formation of droplets is functionally coupled with virus replication [132].

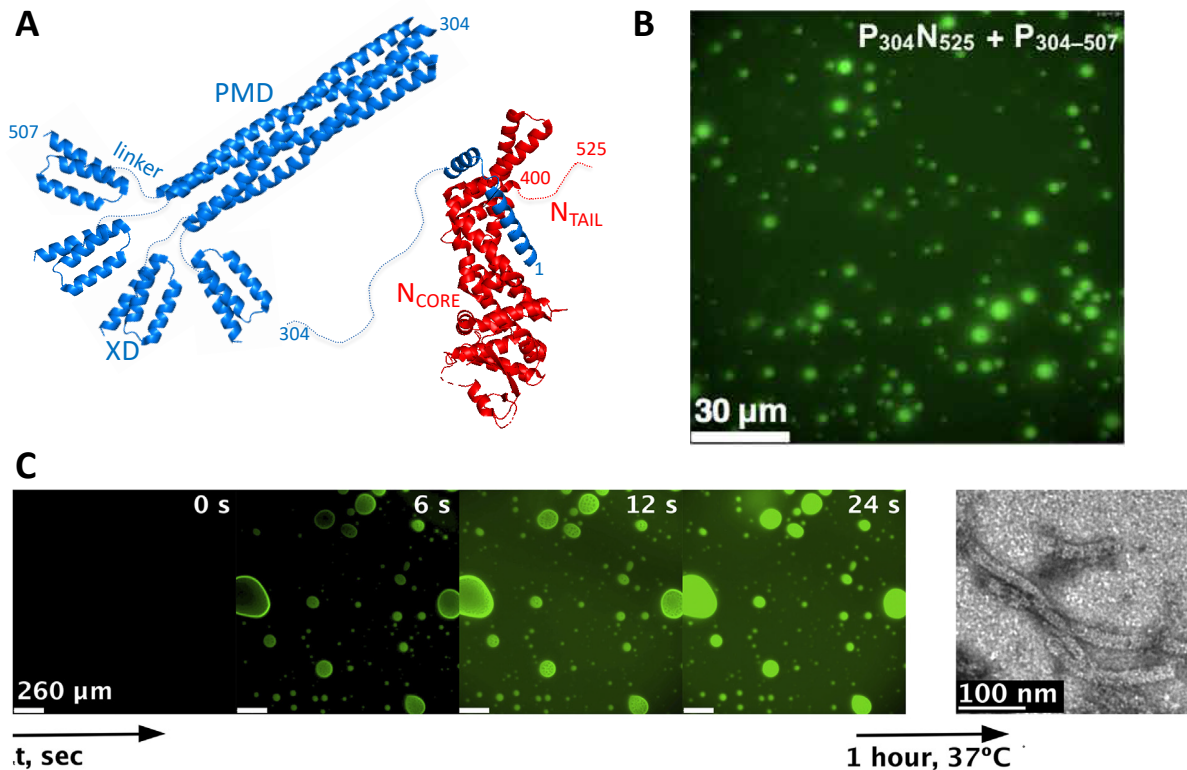


**Figure 6. Phase separating abilities of MeV N and P proteins, RNA colocalization and formation of nucleocapsid-like particles.** (A) Cartoon representation of the MeV P region encompassing residues 304-507 (left) and of the full-length N protein (N<sub>1-525</sub>) in complex with the P region encompassing residues 1-304 (P<sub>1-304</sub>) (right). PDB codes are 3ZDO for PMD [41], 1OKS for XD [21], and 5E4V for the N<sup>o</sup>-P<sub>NT</sub> complex [10]. (B) Fluorescence microscopy image of a mixture containing fluorescein-labeled P<sub>1-304</sub>N<sub>1-525</sub> and P<sub>304-507</sub> under conditions where LLPS occurs. (C) Fluorescence microscopy image showing fluorescently labeled RNA diffusing into droplets preformed by mixing P<sub>1-50</sub>N<sub>1-525</sub> and P<sub>304-507</sub>. RNA colocalizes to N:P droplets and forms nucleocapsid-like particles, as observed by negative-staining electron microscopy after 1 hour of incubation at 37°C. Panels B and C reproduced with permission from [132]. Structures were drawn using Pymol [25].

*Henipavirus* viral factories have only a suspected liquid-like nature, as inferred from their spherical appearance [133], but the formal demonstration has still to be provided. The minimal region of HeV V conferring the ability to phase separate (*i.e.*, PNT3), is also part of the P protein. It is therefore conceivable that *Henipavirus* P can phase separate as well, with this ability being functionally coupled to the formation of viral factories. On the other hand, *Henipavirus* P may also phase separate on its own even in the absence of N, as recently reported for human metapneumovirus P [134].

Beyond their role in the formation of viral factories, IDRs within viral proteins also drive the formation of viral condensates that interfere with (dis)assembly and regulation of host MLOs and hence with host cell functions [122,125]. The formation of fibrillar aggregates by the *Henipavirus* V and W proteins may be functionally coupled to this “LLPS-mediated interference with host cell functions”: fibrillation by V and W could be revisited in light of LLPS, where those fibrils might correspond to solid-like inclusions formed upon the maturation of liquid-like condensates. In light of the critical role of the *Henipavirus* V and W proteins in evading the host innate immune response, and of the biological functions described for the few viral amyloids reported so far (for a review see [122]), it is tempting to

hypothesize that in infected cells PNT3-mediated fibrillar aggregates could sequester key cellular proteins involved in the antiviral response thereby providing examples of LLPS-mediated viral interference with host cell functions through interaction with cellular proteins. Specifically, PNT3-mediated fibrillar aggregates may sequester cellular partners involved in the host innate immune response, such as STAT and 14-3-3 proteins, thereby preventing IFN signaling and abrogating NF- $\kappa$ B-induced proinflammatory response. Likewise, it can be speculated that the ability of NiV W to prevent IFN- $\beta$  expression could be functionally linked to the formation of W amyloids as shown in the case of Rift Valley fever virus NSs amyloids [135].

#### *Disorder as a determinant of interactivity*

Structural disorder is a well-known determinant of protein interactivity, whereby the increased plasticity typical of IDPs/IDRs enables them to engage in a broad molecular partnership [136-138]. In line with this, and owing to its exposure at the surface of the NC [31], MeV N<sub>TAIL</sub> binds to numerous partners. Indeed, beyond XD [21,23,27,28,139], N<sub>TAIL</sub> interacts with the matrix protein [140], and with various cellular proteins including hsp70 [141-143], a nuclear export protein [144], the interferon regulatory factor 3 [145,146], a yet unidentified protein cell receptor involved in MeV-induced immunosuppression [147,148], and peroxiredoxin 1 [149]. In addition, MeV N, likely via N<sub>TAIL</sub>, interacts with cell cytoskeleton components [150,151]. In the case of N<sub>TAIL</sub> from NiV and HeV, an even broader molecular partnership can be expected thanks to the presence of an additional MoRE that could be involved in binding to yet unidentified partners [30,49]. Analysis of the interactome of *Henipavirus* N proteins, as obtained using the INTACT data base [152] and from literature data mining, revealed that while NiV N has as many as 16 protein partners, the HeV N protein has no known interactors except P (**Fig. 7**). This discrepancy likely merely reflects the fact that NiV has been much more intensively studied than HeV. Partners of NiV N are mainly host enzymes with broad functions in metabolism or chaperoning (**Fig. 7**). The high sequence similarity between HeV and NiV N (97%) advocates for a conserved interaction network between the two proteins. Fewer and distinct interactors were retrieved for MeV N compared to NiV N (**Fig. 7**), possibly reflecting the presence of the additional MoRE in NiV N<sub>TAIL</sub> [30,49]. Although MeV and NiV N have a distinct molecular partnership, they share the ability to bind to chaperones like Hsp40 and Hsp70 (**Fig. 7**).

Similarly to N<sub>TAIL</sub>, MeV P<sub>NTD</sub> interacts with multiple partners, including N in both assembled and unassembled forms [9,10,67,153] and cellular proteins such as STAT1 [154]. As mentioned above and detailed in [85], the *Henipavirus* V and W proteins have a very broad interaction network. To which extent is this promiscuity mediated by IDRs? While a few interactions rely on the structured CTD of V, the interaction with 14-3-3 proteins and with importins  $\alpha$ 1 and  $\alpha$ 3 rely on the disordered CTD of W [77,83,84] and binding to STAT1, STAT4 and PLK1 rely on an IDR within the NTD [80,82] (**Fig. 4A**). To ascertain to which extent the promiscuity of the *Henipavirus* V and W proteins is mediated by their intrinsically disordered NTD, we analyzed the interactome of the *Henipavirus* P, V and W proteins and considered the subset of interactions common to the three. We reasoned that the latter likely correspond to interactions relying on their common NTD (**Fig. 7**). Although their interaction network suffers from a bias (*i.e.* only two partners were retrieved for HeV P and much fewer partners were retrieved for HeV V compared to NiV V), a few observations can nevertheless be done: (1) the V and W proteins interact with the largest number of host proteins), (2) NiV P, V and W share 7 partners, including STAT-1, STAT-2 and STAT-4 proteins. Interestingly, their common protein partners are mainly nuclear, particularly found in the nucleolus of cells. The same consideration holds true for the shared partners between the NiV V and W proteins (29 in total), which may also interact with NiV P. (3) A common set of proteins,

consisting of histones (most recurrent) and of STATs and 14-3-3 proteins, are targeted by the NiV V and W proteins and by the HeV W protein, thereby constituting the largest consensus partner set in the *Henipavirus* interactome. This interaction network hints to a role for the shared large disordered region of the *Henipavirus* V and W proteins in binding nuclear components of the host cell. Because the V protein shuttles between the nucleus and the cytoplasm, its ability to bind nuclear proteins might be functionally linked to the export of the latter to the cytoplasm where they might favor virus replication. Beyond sharing protein targets with V and W, the P protein bridges the interaction network of N and that of V/W, which designates P as an expectedly valuable target for antiviral approaches.

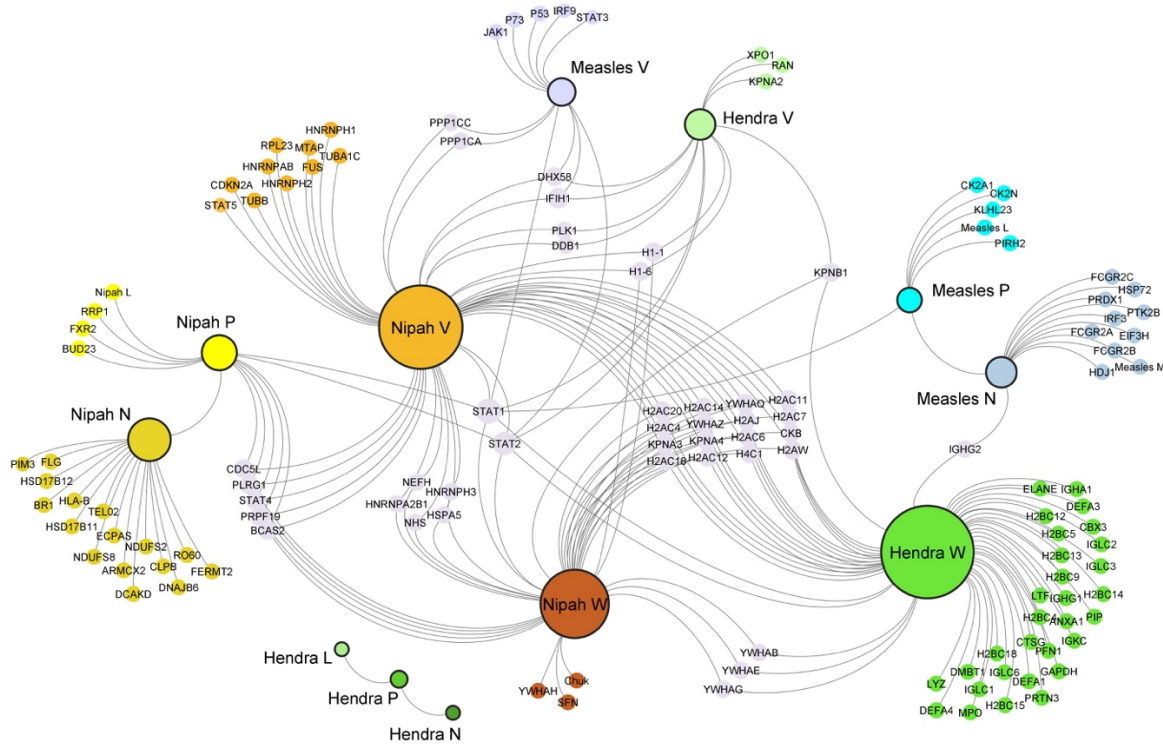


**Figure 7. Interaction network of MeV, NiV and HeV N, P, V and W proteins.** Proteins interacting only with a given viral protein are colored in orange (NiV), green (HeV) and blue (MeV). Shared host partners are shown as pink nodes. Gene names are indicated in nodes and the size of nodes is proportional to the number of protein partners. The figure was drawn using the open source Cytoscape 3.9.1 platform. For additional information see **Supplementary Table S1**.

#### *Disorder as a determinant of scaffolding and tethering*

The typically elongated conformation of IDRs, combined to their very large size (especially for *Henipavirus* P<sub>NTD</sub>), to the multimeric nature of P and to the additional flexibility brought by the “spacer” and “linker” regions of P (**Fig. 1B**), could confer a considerable reach to the elements of the replication machinery enabling them to act as scaffolds for partner tethering. It could also enable the L-P complex to simultaneously bind to successive turns of the helical nucleocapsid (one turn being ~6 nm high [1,155] (**Fig. 1B**). It is tempting to speculate that during replication the extended conformation of P<sub>NTD</sub> and N<sub>TAIL</sub> would allow the establishment of contacts between the assembly substrate (N<sup>o</sup>-P) and the polymerase complex (L-P), leading to a tripartite N<sup>o</sup>-P-L complex. Indeed, since the N<sup>o</sup>-binding site of P does not overlap with the L-binding site, a P molecule engaged in the N<sup>o</sup>-P complex could simultaneously interact with L. This tripartite complex could bring N<sup>o</sup> close to the site of RNA synthesis, where L could promote transfer of N<sup>o</sup> from P to the nascent RNA chain [156]. Alternatively, a monomer of P within the P oligomer may bind to L while another monomer may interact with N<sup>o</sup> thereby bringing the latter

to the encapsidation site [157]. Besides, the flexibility of the “linker” region connecting PMD and XD might serve as a tethering anchor for the recruitment of Hsp90 onto the tripartite complex, thereby enabling L to be maintained in a mature and replication-competent form [5].

#### *Disorder as a lessener of evolutionary constraints*

IDRs are known to be more tolerant of insertions or major rearrangements as compared to ordered regions. In line with this property, the extra-length of *Henipavirus* P proteins with respect to MeV and other paramyxoviruses is accounted for by the larger dimension of their NTD (**Fig. 1B**) [29]. Furthermore, the disordered nature of P<sub>NTD</sub>, whose coding region partially overlaps with the one encoding the C protein, together with the disorder of the “spacer” region, whose coding region partially overlaps with the one encoding V<sub>CTD</sub> [35] (**Fig. 4A**), provides a means for alleviating evolutionary constraints within overlapping open reading frames (OORFs) [158-161].

Because structural disorder is encoded by a much wider portion of sequence space as compared to order, encoding disorder in one of the alternative reading frames may represent a strategy by which genes encoding OORFs can lessen evolutionary constraints imposed on their sequence by the overlap, enabling the encoded overlapping proteins to sample a broader sequence space without losing function.

#### **Conclusions**

Following seminal observations that unveiled the abundance of disorder in paramyxoviral N and P proteins [28,35,162,163], several subsequent studies have documented the prevalence of disorder in many viral proteins [164] and especially in the proteome of RNA viruses (for a review see [165]). As discussed above, structural disorder confers an expanded coding capacity, where a single gene would encode more than one product by means of OORFs. In addition, disorder confers pleiotropy to viral genomes, where a single encoded protein product is able to exert multiple concomitant biological effects thanks to its promiscuity and to the ability of highjacking host proteins through broad mimicry of host protein short linear motifs (SLiMs) [166]. Beyond affording a broad and versatile partnership, and enabling a wide range of phase separation behaviors, the prevalence of IDRs in viral proteins could also be related to the typical high mutation rates of RNA viruses, *i.e.* it could represent a strategy for buffering the deleterious effects of mutations [167,168]. Indeed, IDRs are much less sensitive to mutations compared to structured regions as they have “little to lose”. The mutational tolerance of IDRs is therefore ideally suited to attenuate the potentially detrimental effects of mutations which typically occur at higher rates in viruses [167].

Are there only advantages in being disordered? IDPs/IDRs have an increased vulnerability compared to structured proteins as they are more susceptible to proteolysis [26] and their level needs to be tightly controlled to preserve their specificity and avoid miss-regulation of cellular processes [169-171]. Reflecting this requirement, paramyxoviruses have evolved strategies to finely control the expression level of their own disorder-enriched proteins. Indeed, as already discussed, in the course of evolution the N<sub>TAIL</sub>-XD affinity, which dictates the efficiency of transcription re-initiation and hence ultimately the relative abundance of the different viral proteins, has been shaped to fall into a relatively narrow window [69]. Likewise, evolution has shaped the PMD sequence to endow it with a precise extent of cohesiveness, the latter having been shown to critically affect the efficiency of viral transcription and replication [7].

How does the abundance of structural disorder in viral proteomes translate into therapeutic approaches? The abundance of structural disorder in viral proteins and the complexity of their partnership in infected cells open up new and innovative antiviral strategies relying on the targeting of protein-protein interactions (PPIs) involving IDRs. Targeting PPIs is very attractive since protein

interaction surfaces are much less conserved than catalytic pockets of enzymes thus offering potential for highly specific inhibition. The inhibition of PPIs has thus emerged during the last two decades as a new way to modulate the activity of proteins. That PPIs mediated by IDRs are valuable targets has been already proven [172-179]. Drug-like compounds that target the HIV-1 Nef-SH3 binding surface provided the first “proof of concept” for antiviral discoveries relying on PPI inhibition, thus paving the way towards a new class of antiviral molecules [172]. The relevance of such an approach in antiviral therapies against paramyxoviruses is well illustrated by the antiviral activity of peptides targeting the N<sup>o</sup>-P<sub>NT</sub> interaction from either NiV [9] or RSV [180]. The N<sub>TAIL</sub>-XD interaction is a similarly attractive target as, beyond involving a disordered partner, it is endowed with a number of features that support its potential druggability. Firstly, the rather weak binding affinity of the N<sub>TAIL</sub>-XD interaction (K<sub>D</sub> in the μM range) [30,49,50] is expected to allow tighter competitive binding by small molecule drugs to the structured partner. Secondly, the relatively small size of the N<sub>TAIL</sub>-XD interface area in the three viruses [23,46,181] presages an interaction that is prone to destabilization, in agreement with the commonly accepted relationship between interface buried surface area and complex stability. Thirdly, in spite of the additional role of electrostatics in complex formation [58], the N<sub>TAIL</sub>-XD interface in the three viruses mainly relies on hydrophobic contacts and protein-protein interfaces with known inhibitors are more hydrophobic than general PPI interfaces [182]. Last, but not least, since *Henipavirus* N<sub>TAIL</sub> domains are functionally interchangeable with respect to their ability to bind XD [49], a single inhibitor could probably target both interactions thus paving the way towards a new set of broad-range antivirals.

Finally, and most interestingly, the discovery that a peptide abrogating LLPS by the SARS-CoV2 nucleoprotein leads to increased innate antiviral responses *in vitro* and in mice [183] highlights the potential of targeting LLPS to treat viral infections. In the same vein, LLPS during the replication of human respiratory syncytial virus (RSV, a pneumovirus member within the *Mononegavirales* order) was proven to be a valuable target for antiviral therapy: cyclophamide and its chemical analogue (A3E) were found to inhibit RSV replication in a mouse model of infection by disorganizing and hardening viral IBs that readily lose their liquid-like behavior [184]. The ability of a condensate-hardening drug to inhibit the replication of RSV holds promise for new antiviral approaches based on the pharmacological modulation of the material properties of biocondensates through the targeting of PPIs hitherto considered as undruggable [124].

**Acknowledgments.** S.L. wishes to thank the previous members of her lab for their precious contribution to the studies herein summarized. In particular, she thanks David Karlin, François Ferron, Jean-Marie Bourhis, Kenth Johansson, Antoine Gruet, Johnny Habchi, David Blocquel, Jenny Eroles, Lorenzo Baronti, Marion Dosnon, Jennifer Roche, Matilde Beltrandi, Francesca Troilo, Antoine Schramm and Edoardo Salladini. Among her numerous past and present co-workers, she particularly thanks Stefano Gianni (Sapienza, University of Rome, Italy), Roberta Pierattelli and Isabella Felli (CERM, University of Florence, Italy) and Louis-Marie Bloyet (Molecular Microbiology Department, Washington University, St. Louis, Missouri, USA). The studies herein summarized were carried out with the financial support of the Agence Nationale de la Recherche, specific programs Physico-Chimie du Vivant, ANR-08-PCVI-0020-01, ASTRID, ANR-11-ASTR-003-01 and specific project Heniphase (ANR-21-CE11-0012-01) to S.L. We also thank the Lyon Biopole and Eurobiomed competitiveness poles for labeling the ANR Heniphase project. The studies herein reviewed also benefited from support from the CNRS and the Direction Générale de l’Armement (DGA). F. G. is supported by a post-doctoral fellowship from the FRM. G. P.

is supported by a joint doctoral fellowship from the AID (Agence Innovation Défense) and Aix-Marseille University. J.F.N. is supported by a post-doctoral fellowship from the Infectiopôle Sud.

## References

1. Gutsche, I.; Desfosses, A.; Effantin, G.; Ling, W.L.; Haupt, M.; Ruigrok, R.W.; Sachse, C.; Schoehn, G. Near-atomic cryo-EM structure of the helical measles virus nucleocapsid. *Science* **2015**, *348*, doi:10.1126/science.aaa5137.
2. Ker, D.S.; Jenkins, H.T.; Greive, S.J.; Antson, A.A. CryoEM structure of the Nipah virus nucleocapsid assembly. *PLoS Pathog* **2021**, *17*, e1009740, doi:10.1371/journal.ppat.1009740.
3. Liang, B. Structures of the Mononegavirales Polymerases. *J. Virol.* **2020**, *94*, doi:10.1128/jvi.00175-20.
4. Pyle, J.D.; Whelan, S.P.J.; Bloyet, L.M. Structure and function of negative-strand RNA virus polymerase complexes. *Enzymes* **2021**, *50*, 21-78, doi:10.1016/bs.enz.2021.09.002.
5. Bloyet, L.M.; Welsch, J.; Enchery, F.; Mathieu, C.; de Breyne, S.; Horvat, B.; Grigorov, B.; Gerlier, D. HSP90 Chaperoning in Addition to Phosphoprotein Required for Folding but Not for Supporting Enzymatic Activities of Measles and Nipah Virus L Polymerases. *J. Virol.* **2016**, *90*, 6642-6656, doi:10.1128/JVI.00602-16.
6. Abdella, R.; Aggarwal, M.; Okura, T.; Lamb, R.A.; He, Y. Structure of a paramyxovirus polymerase complex reveals a unique methyltransferase-CTD conformation. *Proc Natl Acad Sci U S A* **2020**, *117*, 4931-4941, doi:10.1073/pnas.1919837117.
7. Bloyet, L.M.; Schramm, A.; Lazert, C.; Raynal, B.; Hologne, M.; Walker, O.; Longhi, S.; Gerlier, D. Regulation of measles virus gene expression by P protein coiled-coil properties. *Sci Adv* **2019**, *5*, eaaw3702, doi:10.1126/sciadv.aaw3702.
8. Brunel, J.; Chopy, D.; Dosnon, M.; Bloyet, L.M.; Devaux, P.; Urzua, E.; Cattaneo, R.; Longhi, S.; Gerlier, D. Sequence of events in measles virus replication: role of phosphoprotein-nucleocapsid interactions. *J. Virol.* **2014**, *88*, 10851-10863, doi:10.1128/JVI.00664-14.
9. Yabukarski, F.; Lawrence, P.; Tarbouriech, N.; Bourhis, J.M.; Delaforge, E.; Jensen, M.R.; Ruigrok, R.W.; Blackledge, M.; Volchkov, V.; Jamin, M. Structure of Nipah virus unassembled nucleoprotein in complex with its viral chaperone. *Nat. Struct. Mol. Biol.* **2014**, *21*, 754-759, doi:10.1038/nsmb.2868.
10. Guryanov, S.G.; Liljeroos, L.; Kasaragod, P.; Kajander, T.; Butcher, S.J. Crystal Structure of the Measles Virus Nucleoprotein Core in complex with an N-terminal Region of Phosphoprotein. *J. Virol.* **2016**, *90*, 2849–2857, doi:10.1128/JVI.02865-15.
11. Milles, S.; Jensen, M.R.; Communie, G.; Maurin, D.; Schoehn, G.; Ruigrok, R.W.; Blackledge, M. Self-Assembly of Measles Virus Nucleocapsid-like Particles: Kinetics and RNA Sequence Dependence. *Angew Chem Int Ed Engl* **2016**, *55*, 9356-9360, doi:10.1002/anie.201602619.
12. Desfosses, A.; Milles, S.; Jensen, M.R.; Guseva, S.; Colletier, J.P.; Maurin, D.; Schoehn, G.; Gutsche, I.; Ruigrok, R.W.H.; Blackledge, M. Assembly and cryo-EM structures of RNA-specific measles virus nucleocapsids provide mechanistic insight into paramyxoviral replication. *Proc Natl Acad Sci U S A* **2019**, doi:10.1073/pnas.1816417116.
13. Longhi, S. Nucleocapsid structure and function. *Curr Top Microbiol Immunol* **2009**, *329*, 103-128.
14. Longhi, S.; Oglesbee, M. Structural disorder within the measles virus nucleoprotein and phosphoprotein. *Protein and Peptide Letters* **2010**, *17*, 961-978, doi:10.2174/092986610791498894.
15. Blocquel, D.; Bourhis, J.M.; Eléouët, J.F.; Gerlier, D.; Habchi, J.; Jamin, M.; Longhi, S.; Yabukarski, F. Transcription et répllication des Mononégavirales: une machine moléculaire originale. *Virologie* **2012**, *16*, 225-257, doi:10.1684/vir.2012.0458.
16. Habchi, J.; Longhi, S. Structural Disorder within Paramyxoviral Nucleoproteins and Phosphoproteins in Their Free and Bound Forms: From Predictions to Experimental Assessment. *Int J Mol Sci* **2015**, *16*, 15688-15726, doi:10.3390/ijms160715688.
17. Longhi, S. Structural disorder within paramyxoviral nucleoproteins. *FEBS Lett.* **2015**, *589*, 2649-2659, doi:10.1016/j.febslet.2015.05.055.

18. Eralles, J.; Blocquel, D.; Habchi, J.; Beltrandi, M.; Gruet, A.; Dosnon, M.; Bignon, C.; Longhi, S. Order and disorder in the replicative complex of paramyxoviruses. *Adv. Exp. Med. Biol.* **2015**, *870*, 351-381, doi:10.1007/978-3-319-20164-1\_12.
19. Longhi, S.; Bloyet, L.M.; Gianni, S.; Gerlier, D. How order and disorder within paramyxoviral nucleoproteins and phosphoproteins orchestrate the molecular interplay of transcription and replication. *Cell. Mol. Life Sci.* **2017**, *74*, 3091-3118, doi:10.1007/s00018-017-2556-3.
20. Bloyet, L.M. The Nucleocapsid of Paramyxoviruses: Structure and Function of an Encapsidated Template. *Viruses* **2021**, *13*, doi:10.3390/v13122465.
21. Johansson, K.; Bourhis, J.M.; Campanacci, V.; Cambillau, C.; Canard, B.; Longhi, S. Crystal structure of the measles virus phosphoprotein domain responsible for the induced folding of the C-terminal domain of the nucleoprotein. *J. Biol. Chem.* **2003**, *278*, 44567-44573.
22. Blocquel, D.; Habchi, J.; Durand, E.; Sevajol, M.; Ferron, F.; Eralles, J.; Papageorgiou, N.; Longhi, S. Coiled-coil deformations in crystal structures: the measles virus phosphoprotein multimerization domain as an illustrative example. *Acta Cryst D* **2014**, *70*, 1589-1603.
23. Kingston, R.L.; Hamel, D.J.; Gay, L.S.; Dahlquist, F.W.; Matthews, B.W. Structural basis for the attachment of a paramyxoviral polymerase to its template. *Proc Natl Acad Sci U S A* **2004**, *101*, 8301-8306.
24. Lazar, T.; Martínez-Pérez, E.; Quaglia, F.; Hatos, A.; Chemes, L.B.; Iserte, J.A.; Méndez, N.A.; Garrone, N.A.; Saldaño, T.E.; Marchetti, J.; et al. PED in 2021: a major update of the protein ensemble database for intrinsically disordered proteins. *Nucleic Acids Res.* **2021**, *49*, D404-d411, doi:10.1093/nar/gkaa1021.
25. DeLano, W.L. The PyMOL molecular graphics system *Proteins: Structure, Function and Bioinformatics* **2002**, *30*, 442-454.
26. Habchi, J.; Tompa, P.; Longhi, S.; Uversky, V.N. Introducing Protein Intrinsic Disorder. *Chem Rev* **2014**, *114*, 6561-6588, doi:10.1021/cr400514h.
27. Bourhis, J.; Johansson, K.; Receveur-Bréchet, V.; Oldfield, C.J.; Dunker, A.K.; Canard, B.; Longhi, S. The C-terminal domain of measles virus nucleoprotein belongs to the class of intrinsically disordered proteins that fold upon binding to their physiological partner. *Virus Res.* **2004**, *99*, 157-167.
28. Longhi, S.; Receveur-Brechot, V.; Karlin, D.; Johansson, K.; Darbon, H.; Bhella, D.; Yeo, R.; Finet, S.; Canard, B. The C-terminal domain of the measles virus nucleoprotein is intrinsically disordered and folds upon binding to the C-terminal moiety of the phosphoprotein. *J. Biol. Chem.* **2003**, *278*, 18638-18648., doi: 10.1074/jbc.M300518200.
29. Habchi, J.; Mamelli, L.; Darbon, H.; Longhi, S. Structural Disorder within Henipavirus Nucleoprotein and Phosphoprotein: From Predictions to Experimental Assessment. *PLoS ONE* **2010**, *5*, e11684, doi:10.1371/journal.pone.0011684.
30. Habchi, J.; Blangy, S.; Mamelli, L.; Ringkjøbing Jensen, M.; Blackledge, M.; Darbon, H.; Oglesbee, M.; Shu, Y.; Longhi, S. Characterization of the interactions between the nucleoprotein and the phosphoprotein of Henipaviruses. *J. Biol. Chem.* **2011**, *286*, 13583-13602, doi:10.1074/jbc.M111.219857
31. Ringkjøbing Jensen, M.; Communie, G.; Ribeiro, E.D., Jr.; Martinez, N.; Desfosses, A.; Salmon, L.; Mollica, L.; Gabel, F.; Jamin, M.; Longhi, S.; et al. Intrinsic disorder in measles virus nucleocapsids. *Proc Natl Acad Sci U S A* **2011**, *108*, 9839-9844.
32. Communie, G.; Habchi, J.; Yabukarski, F.; Blocquel, D.; Schneider, R.; Tarbouriech, N.; Papageorgiou, N.; Ruigrok, R.W.; Jamin, M.; Ringkjøbing-Jensen, M.; et al. Atomic resolution description of the interaction between the nucleoprotein and phosphoprotein of Hendra virus. *PLoS Pathog* **2013**, *9*, e1003631, doi:e1003631.
33. Baronti, L.; Eralles, J.; Habchi, J.; Felli, I.C.; Pierattelli, R.; Longhi, S. Dynamics of the intrinsically disordered C-terminal domain of the Nipah virus nucleoprotein and interaction with the X domain of the phosphoprotein as unveiled by NMR spectroscopy. *Chem BioChem* **2015**, *16*, 268-276, doi:10.1002/cbic.201402534.

34. Karlin, D.; Longhi, S.; Receveur, V.; Canard, B. The N-terminal domain of the phosphoprotein of Morbilliviruses belongs to the natively unfolded class of proteins. *Virology* **2002**, *296*, 251-262, doi:10.1006/viro.2001.1296.
35. Karlin, D.; Ferron, F.; Canard, B.; Longhi, S. Structural disorder and modular organization in Paramyxovirinae N and P. *J. Gen. Virol.* **2003**, *84*, 3239-3252, doi:10.1099/vir.0.19451-0
36. Jensen, M.R.; Yabukarski, F.; Communie, G.; Condamine, E.; Mas, C.; Volchkova, V.; Tarbouriech, N.; Bourhis, J.M.; Volchkov, V.; Blackledge, M.; et al. Structural Description of the Nipah Virus Phosphoprotein and Its Interaction with STAT1. *Biophys. J.* **2020**, *118*, 2470-2488, doi:10.1016/j.bpj.2020.04.010.
37. Schiavina, M.; Salladini, E.; Murralli, M.G.; Tria, G.; Felli, I.C.; Pierattelli, R.; Longhi, S. Ensemble description of the intrinsically disordered N-terminal domain of the Nipah virus P/V protein from combined NMR and SAXS. *Sci Rep* **2020**, *10*, 19574, doi:10.1038/s41598-020-76522-3.
38. Milles, S.; Jensen, M.R.; Lazert, C.; Guseva, S.; Ivashchenko, S.; Communie, G.; Maurin, D.; Gerlier, D.; Ruigrok, R.W.H.; Blackledge, M. An ultraweak interaction in the intrinsically disordered replication machinery is essential for measles virus function. *Sci Adv* **2018**, *4*, eaat7778, doi:10.1126/sciadv.aat7778.
39. Du Pont, V.; Jiang, Y.; Plemper, R.K. Bipartite interface of the measles virus phosphoprotein X domain with the large polymerase protein regulates viral polymerase dynamics. *PLoS Pathog* **2019**, *15*, e1007995, doi:10.1371/journal.ppat.1007995.
40. Bruhn-Johannsen, J.F.; Barnett, K.; Bibby, J.; Thomas, J.; Keegan, R.; Rigden, D.; Bornholdt, Z.A.; Saphire, E.O. Crystal structure of the Nipah virus phosphoprotein tetramerization domain. *J. Virol.* **2014**, *88*, 758-762, doi:10.1128/JVI.02294-13.
41. Communie, G.; Crepin, T.; Maurin, D.; Jensen, M.R.; Blackledge, M.; Ruigrok, R.W. Structure of the tetramerization domain of measles virus phosphoprotein. *J. Virol.* **2013**, *87*, 7166-7169, doi:10.1128/JVI.00487-13.
42. Blocquel, D.; Beltrandi, M.; Eroles, J.; Barbier, P.; Longhi, S. Biochemical and structural studies of the oligomerization domain of the Nipah virus phosphoprotein: Evidence for an elongated coiled-coil homotrimer. *Virology* **2013**, *446*, 162-172, doi:10.1016/j.virol.2013.07.031.
43. Beltrandi, M.; Blocquel, D.; Eroles, J.; Barbier, P.; Cavalli, A.; Longhi, S. Insights into the coiled-coil organization of the Hendra virus phosphoprotein from combined biochemical and SAXS studies. *Virology* **2015**, *477*, 42-55, doi:10.1016/j.virol.2014.12.029.
44. D'Urzo, A.; Konijnenberg, A.; Rossetti, G.; Habchi, J.; Li, J.; Carloni, P.; Sobott, F.; Longhi, S.; Grandori, R. Molecular Basis for Structural Heterogeneity of an Intrinsically Disordered Protein Bound to a Partner by Combined ESI-IM-MS and Modeling. *J. Am. Soc. Mass Spectrom.* **2015**, *26*, 472-481, doi:10.1007/s13361-014-1048-z.
45. Bonetti, D.; Camilloni, C.; Visconti, L.; Longhi, S.; Brunori, M.; Vendruscolo, M.; Gianni, S. Identification and Structural Characterization of an Intermediate in the Folding of the Measles Virus X Domain. *J. Biol. Chem.* **2016**, *291*, 10886-10892, doi:10.1074/jbc.M116.721126.
46. Bourhis, J.M.; Yabukarski, F.; Communie, G.; Schneider, R.; Volchkova, V.A.; Frén at, M.; G erard, F.; Ducournau, C.; Mas, C.; Tarbouriech, N.; et al. Structural dynamics of the C-terminal X domain of Nipah and Hendra viruses controls the attachment to the C-terminal tail of the nucleocapsid protein. *J. Mol. Biol.* **2022**, 167551, doi:10.1016/j.jmb.2022.167551.
47. Kingston, R.L.; Gay, L.S.; Baase, W.S.; Matthews, B.W. Structure of the nucleocapsid-binding domain from the mumps virus polymerase; an example of protein folding induced by crystallization. *J. Mol. Biol.* **2008**, *379*, 719-731, doi:10.1016/j.jmb.2007.12.080.
48. Yegambaram, K.; Bulloch, E.M.; Kingston, R.L. Protein domain definition should allow for conditional disorder. *Protein Sci.* **2013**, *22*, 1502-1518, doi:10.1002/pro.2336.
49. Blocquel, D.; Habchi, J.; Gruet, A.; Blangy, S.; Longhi, S. Compaction and binding properties of the intrinsically disordered C-terminal domain of Henipavirus nucleoprotein as unveiled by deletion studies. *Mol Biosyst* **2012**, *8*, 392-410, doi:10.1039/c1mb05401e.

50. Dosnon, M.; Bonetti, D.; Morrone, A.; Eroles, J.; di Silvio, E.; Longhi, S.; Gianni, S. Demonstration of a folding after binding mechanism in the recognition between the measles virus NTAIL and X domains. *ACS ChemBiol* **2015**, *10*, 795-802.
51. Belle, V.; Rouger, S.; Costanzo, S.; Liquiere, E.; Strancar, J.; Guigliarelli, B.; Fournel, A.; Longhi, S. Mapping alpha-helical induced folding within the intrinsically disordered C-terminal domain of the measles virus nucleoprotein by site-directed spin-labeling EPR spectroscopy. *Proteins: Structure, Function and Bioinformatics* **2008**, *73*, 973-988, doi:10.1002/prot.22125.
52. Gely, S.; Lowry, D.F.; Bernard, C.; Ringkjober-Jensen, M.; Blackledge, M.; Costanzo, S.; Darbon, H.; Daughdrill, G.W.; Longhi, S. Solution structure of the C-terminal X domain of the measles virus phosphoprotein and interaction with the intrinsically disordered C-terminal domain of the nucleoprotein *J Mol Recognit* **2010**, *23*, 435-447.
53. Morin, B.; Bourhis, J.M.; Belle, V.; Woudstra, M.; Carrière, F.; Guigliarelli, B.; Fournel, A.; Longhi, S. Assessing induced folding of an intrinsically disordered protein by site-directed spin-labeling EPR spectroscopy. *J. Phys. Chem. B* **2006**, *110*, 20596-20608.
54. Bischak, C.G.; Longhi, S.; Snead, D.M.; Costanzo, S.; Terror, E.; Londergan, C.H. Probing structural transitions in the intrinsically disordered C-terminal domain of the measles virus nucleoprotein by vibrational spectroscopy of cyanylated cysteines. *Biophys. J.* **2010**, *99*, 1676-1683.
55. Martinho, M.; Habchi, J.; El Habre, Z.; Nesme, L.; Guigliarelli, B.; Belle, V.; Longhi, S. Assessing induced folding within the intrinsically disordered C-terminal domain of the Henipavirus nucleoproteins by site directed spin labeling EPR spectroscopy. *J. Biomol. Struct. Dyn.* **2013**, *31*, 453-471, doi: 10.1080/07391102.2012.706068
56. Wang, Y.; Chu, X.; Longhi, S.; Roche, P.; Han, W.; Wang, E.; Wang, J. Multiscaled exploration of coupled folding and binding of an intrinsically disordered molecular recognition element in measles virus nucleoprotein. *Proc Natl Acad Sci U S A* **2013**, *110*, E3743-E3752, doi:10.1073/pnas.1308381110.
57. Bonetti, D.; Troilo, F.; Toto, A.; Brunori, M.; Longhi, S.; Gianni, S. Analyzing the folding and binding steps of an intrinsically disordered protein by protein engineering. *Biochemistry* **2017**, *56*, 3780-3786.
58. Eroles, J.; Beltrandi, M.; Roche, J.; Maté, M.; Longhi, S. Insights into the Hendra virus NTAIL-XD complex: Evidence for a parallel organization of the helical MoRE at the XD surface stabilized by a combination of hydrophobic and polar interactions. *Biochim Biophys Acta* **2015**, *1854*, 1038-1053, doi:10.1016/j.bbapap.2015.04.031.
59. Fuxreiter, M.; Tompa, P. Fuzzy complexes: a more stochastic view of protein function. *Adv. Exp. Med. Biol.* **2012**, *725*, 1-14, doi:10.1007/978-1-4614-0659-4\_1.
60. Bourhis, J.M.; Receveur-Bréchet, V.; Oglesbee, M.; Zhang, X.; Buccellato, M.; Darbon, H.; Canard, B.; Finet, S.; Longhi, S. The intrinsically disordered C-terminal domain of the measles virus nucleoprotein interacts with the C-terminal domain of the phosphoprotein via two distinct sites and remains predominantly unfolded. *Protein Sci.* **2005**, *14*, 1975-1992, doi:10.1110/ps.051411805.
61. Kavalenka, A.; Urbancic, I.; Belle, V.; Rouger, S.; Costanzo, S.; Kure, S.; Fournel, A.; Longhi, S.; Guigliarelli, B.; Strancar, J. Conformational analysis of the partially disordered measles virus N(TAIL)-XD complex by SDSL EPR spectroscopy. *Biophys. J.* **2010**, *98*, 1055-1064, doi:10.1016/j.bpj.2009.11.036.
62. Gruet, A.; Dosnon, M.; Blocquel, D.; Brunel, J.; Gerlier, D.; Das, R.K.; Bonetti, D.; Gianni, S.; Fuxreiter, M.; Longhi, S.; et al. Fuzzy regions in an intrinsically disordered protein impair protein-protein interactions. *FEBS J.* **2016**, *283*, 576-594, doi:10.1111/febs.13631.
63. Troilo, F.; Bonetti, D.; Bignon, C.; Longhi, S.; Gianni, S. Understanding Intramolecular Crosstalk in an Intrinsically Disordered Protein. *ACS Chem Biol* **2019**, *14*, 337-341, doi:10.1021/acscchembio.8b01055.

64. Bignon, C.; Troilo, F.; Gianni, S.; Longhi, S. Partner-Mediated Polymorphism of an Intrinsically Disordered Protein. *J. Mol. Biol.* **2018**, *430*, 2493-2507, doi:10.1016/j.jmb.2017.11.012.
65. Kolakofsky, D.; Le Mercier, P.; Iseni, F.; Garcin, D. Viral DNA polymerase scanning and the gymnastics of Sendai virus RNA synthesis. *Virology* **2004**, *318*, 463-473.
66. Cox, R.M.; Krumm, S.A.; Thakkar, V.D.; Sohn, M.; Plemper, R.K. The structurally disordered paramyxovirus nucleocapsid protein tail domain is a regulator of the mRNA transcription gradient. *Sci Adv* **2017**, *3*, e1602350, doi:10.1126/sciadv.1602350.
67. Krumm, S.A.; Takeda, M.; Plemper, R.K. The measles virus nucleocapsid protein tail domain is dispensable for viral polymerase recruitment and activity. *J. Biol. Chem.* **2013**, *288*, 29943-29953, doi:10.1074/jbc.M113.503862.
68. Gruet, A.; Dosnon, M.; Vassena, A.; Lombard, V.; Gerlier, D.; Bignon, C.; Longhi, S. Dissecting partner recognition by an intrinsically disordered protein using descriptive random mutagenesis. *J. Mol. Biol.* **2013**, *425*, 3495-3509, doi:10.1016/j.jmb.2013.06.025.
69. Bloyet, L.M.; Brunel, J.; Dosnon, M.; Hamon, V.; Erales, J.; Gruet, A.; Lazert, C.; Bignon, C.; Roche, P.; Longhi, S.; et al. Modulation of Re-initiation of Measles Virus Transcription at Intergenic Regions by PXD to NTAIL Binding Strength. *PLoS Pathog* **2016**, *12*, e1006058, doi:10.1371/journal.ppat.1006058.
70. Douglas, J.; Drummond, A.J.; Kingston, R.L. Evolutionary history of cotranscriptional editing in the paramyxoviral phosphoprotein gene. *Virus Evolution* **2021**, *7*, doi:10.1093/ve/veab028.
71. Fontana, J.M.; Bankamp, B.; Rota, P.A. Inhibition of interferon induction and signaling by paramyxoviruses. *Immunol. Rev.* **2008**, *225*, 46-67, doi:10.1111/j.1600-065X.2008.00669.x.
72. Audsley, M.D.; Moseley, G.W. Paramyxovirus evasion of innate immunity: Diverse strategies for common targets. *World J Virol* **2013**, *2*, 57-70, doi:10.5501/wjv.v2.i2.57.
73. Tsimbalyuk, S.; Cross, E.M.; Hoad, M.; Donnelly, C.M.; Roby, J.A.; Forwood, J.K. The Intrinsically Disordered W Protein Is Multifunctional during Henipavirus Infection, Disrupting Host Signalling Pathways and Nuclear Import. *Cells* **2020**, *9*, doi:10.3390/cells9081913.
74. Ulane, C.M.; Horvath, C.M. Paramyxoviruses SV5 and HPIV2 assemble STAT protein ubiquitin ligase complexes from cellular components. *Virology* **2002**, *304*, 160-166, doi:10.1006/viro.2002.1773.
75. Salladini, E.; Delauzun, V.; Longhi, S. The Henipavirus V protein is a prevalently unfolded protein with a zinc-finger domain involved in binding to DDB1. *Mol Biosyst* **2017**, *13*, 2254-2267, doi:10.1039/c7mb00488e.
76. Shaw, M.L.; Garcia-Sastre, A.; Palese, P.; Basler, C.F. Nipah virus V and W proteins have a common STAT1-binding domain yet inhibit STAT1 activation from the cytoplasmic and nuclear compartments, respectively. *J. Virol.* **2004**, *78*, 5633-5641, doi:10.1128/JVI.78.11.5633-5641.2004.
77. Smith, K.M.; Tsimbalyuk, S.; Edwards, M.R.; Cross, E.M.; Batra, J.; Soares da Costa, T.P.; Aragao, D.; Basler, C.F.; Forwood, J.K. Structural basis for importin alpha 3 specificity of W proteins in Hendra and Nipah viruses. *Nat Commun* **2018**, *9*, 3703, doi:10.1038/s41467-018-05928-5.
78. Audsley, M.D.; Jans, D.A.; Moseley, G.W. Nucleocytoplasmic trafficking of Nipah virus W protein involves multiple discrete interactions with the nuclear import and export machinery. *Biochem. Biophys. Res. Commun.* **2016**, *479*, 429-433, doi:10.1016/j.bbrc.2016.09.043.
79. Pichlmair, A.; Kandasamy, K.; Alvisi, G.; Mulhern, O.; Sacco, R.; Habjan, M.; Binder, M.; Stefanovic, A.; Eberle, C.A.; Goncalves, A.; et al. Viral immune modulators perturb the human molecular network by common and unique strategies. *Nature* **2012**, *487*, 486-490, doi:10.1038/nature11289.
80. Keiffer, T.R.; Ciancanelli, M.J.; Edwards, M.R.; Basler, C.F. Interactions of the Nipah Virus P, V, and W Proteins across the STAT Family of Transcription Factors. *mSphere* **2020**, *5*, doi:10.1128/mSphere.00449-20.
81. Childs, K.; Randall, R.; Goodbourn, S. Paramyxovirus V proteins interact with the RNA Helicase LGP2 to inhibit RIG-I-dependent interferon induction. *J. Virol.* **2012**, *86*, 3411-3421, doi:10.1128/JVI.06405-11.

82. Ludlow, L.E.; Lo, M.K.; Rodriguez, J.J.; Rota, P.A.; Horvath, C.M. Henipavirus V protein association with Polo-like kinase reveals functional overlap with STAT1 binding and interferon evasion. *J. Virol.* **2008**, *82*, 6259-6271, doi:10.1128/JVI.00409-08.
83. Edwards, M.R.; Hoad, M.; Tsimbalyuk, S.; Menicucci, A.R.; Messaoudi, I.; Forwood, J.K.; Basler, C.F. Henipavirus W Proteins Interact with 14-3-3 To Modulate Host Gene Expression. *J. Virol.* **2020**, *94*, doi:10.1128/jvi.00373-20.
84. Enchery, F.; Dumont, C.; Iampietro, M.; Pelissier, R.; Aurine, N.; Bloyet, L.M.; Carbonelle, C.; Mathieu, C.; Journo, C.; Gerlier, D.; et al. Nipah virus W protein harnesses nuclear 14-3-3 to inhibit NF- $\kappa$ B-induced proinflammatory response. *Commun Biology* **2021**, *4*, 1292.
85. Pesce, G.; Gondelaud, F.; Ptchelkine, D.; Nilsson, J.F.; Bignon, C.; Cartalas, J.; Fourquet, P.; Longhi, S. Experimental Evidence of Intrinsic Disorder and Amyloid Formation by the Henipavirus W Proteins. *Int J Mol Sci* **2022**, *23*, doi:10.3390/ijms23020923.
86. Holehouse, A.S.; Pappu, R.V. Functional Implications of Intracellular Phase Transitions. *Biochemistry* **2018**, *57*, 2415-2423, doi:10.1021/acs.biochem.7b01136.
87. Alberti, S.; Hyman, A.A. Biomolecular condensates at the nexus of cellular stress, protein aggregation disease and ageing. *Nat. Rev. Mol. Cell Biol.* **2021**, *22*, 196-213, doi:10.1038/s41580-020-00326-6.
88. Fare, C.M.; Villani, A.; Drake, L.E.; Shorter, J. Higher-order organization of biomolecular condensates. *Open Biol* **2021**, *11*, 210137, doi:10.1098/rsob.210137.
89. Shin, Y.; Brangwynne, C.P. Liquid phase condensation in cell physiology and disease. *Science* **2017**, *357*, doi:10.1126/science.aaf4382.
90. Tsang, B.; Pritišanac, I.; Scherer, S.W.; Moses, A.M.; Forman-Kay, J.D. Phase Separation as a Missing Mechanism for Interpretation of Disease Mutations. *Cell* **2020**, *183*, 1742-1756, doi:10.1016/j.cell.2020.11.050.
91. Alberti, S.; Gladfelter, A.; Mittag, T. Considerations and Challenges in Studying Liquid-Liquid Phase Separation and Biomolecular Condensates. *Cell* **2019**, *176*, 419-434, doi:10.1016/j.cell.2018.12.035.
92. Tayeb-Fligelman, E.; Cheng, X.; Tai, C.; Bowler, J.T.; Griner, S.; Sawaya, M.R.; Seidler, P.M.; Jiang, Y.X.; Lu, J.; Rosenberg, G.M.; et al. Inhibition of amyloid formation of the Nucleoprotein of SARS-CoV-2. *bioRxiv* **2021**, doi:10.1101/2021.03.05.434000.
93. Murray, D.T.; Kato, M.; Lin, Y.; Thurber, K.R.; Hung, I.; McKnight, S.L.; Tycko, R. Structure of FUS Protein Fibrils and Its Relevance to Self-Assembly and Phase Separation of Low-Complexity Domains. *Cell* **2017**, *171*, 615-627 e616, doi:10.1016/j.cell.2017.08.048.
94. Uversky, V.N. The roles of intrinsic disorder-based liquid-liquid phase transitions in the "Dr. Jekyll-Mr. Hyde" behavior of proteins involved in amyotrophic lateral sclerosis and frontotemporal lobar degeneration. *Autophagy* **2017**, *13*, 2115-2162, doi:10.1080/15548627.2017.1384889.
95. Patel, A.; Lee, H.O.; Jawerth, L.; Maharana, S.; Jahnel, M.; Hein, M.Y.; Stoyanov, S.; Mahamid, J.; Saha, S.; Franzmann, T.M.; et al. A Liquid-to-Solid Phase Transition of the ALS Protein FUS Accelerated by Disease Mutation. *Cell* **2015**, *162*, 1066-1077, doi:10.1016/j.cell.2015.07.047.
96. Molliex, A.; Temirov, J.; Lee, J.; Coughlin, M.; Kanagaraj, A.P.; Kim, H.J.; Mittag, T.; Taylor, J.P. Phase separation by low complexity domains promotes stress granule assembly and drives pathological fibrillization. *Cell* **2015**, *163*, 123-133, doi:10.1016/j.cell.2015.09.015.
97. Kato, M.; Han, T.W.; Xie, S.; Shi, K.; Du, X.; Wu, L.C.; Mirzaei, H.; Goldsmith, E.J.; Longgood, J.; Pei, J.; et al. Cell-free formation of RNA granules: low complexity sequence domains form dynamic fibers within hydrogels. *Cell* **2012**, *149*, 753-767, doi:10.1016/j.cell.2012.04.017.
98. Boeynaems, S.; Alberti, S.; Fawzi, N.L.; Mittag, T.; Polymenidou, M.; Rousseau, F.; Schymkowitz, J.; Shorter, J.; Wolozin, B.; Van Den Bosch, L.; et al. Protein Phase Separation: A New Phase in Cell Biology. *Trends Cell Biol.* **2018**, *28*, 420-435, doi:10.1016/j.tcb.2018.02.004.
99. Wu, H.; Fuxreiter, M. The Structure and Dynamics of Higher-Order Assemblies: Amyloids, Signalosomes, and Granules. *Cell* **2016**, *165*, 1055-1066, doi:10.1016/j.cell.2016.05.004.

100. Fuxreiter, M.; Vendruscolo, M. Generic nature of the condensed states of proteins. *Nat. Cell Biol.* **2021**, *23*, 587-594, doi:10.1038/s41556-021-00697-8.
101. Salladini, E.; Debarnot, C.; Delauzun, V.; Murralli, M.G.; Sutto-Ortiz, P.; Spinelli, S.; Pierattelli, R.; Bignon, C.; Longhi, S. Phase transition and amyloid formation by a viral protein as an additional molecular mechanism of virus-induced cell toxicity. *BioRxiv* **2018**, 497024, doi:<https://doi.org/10.1101/497024>
102. Salladini, E.; Gondelaud, F.; Nilsson, J.; Pesce, G.; Bignon, C.; Murralli, M.G.; Horvat, B.; Fabre, R.; Pierattelli, R.; Kajava, A.V.; et al. Identification of a region in the common amino-terminal domain of Hendra virus P, V and W proteins responsible for phase transition and amyloid formation. *Biomolecules* **2021**, *11*, 1324, doi:10.3390/biom11091324.
103. Pintado-Grima, C.; Bárcenas, O.; Manglano-Artuñedo, Z.; Vilaça, R.; Macedo-Ribeiro, S.; Pallarès, I.; Santos, J.; Ventura, S. CARs-DB: A Database of Cryptic Amyloidogenic Regions in Intrinsically Disordered Proteins. *Front Mol Biosci* **2022**, *9*, 882160, doi:10.3389/fmolb.2022.882160.
104. Atkinson, S.C.; Audsley, M.D.; Lieu, K.G.; Marsh, G.A.; Thomas, D.R.; Heaton, S.M.; Paxman, J.J.; Wagstaff, K.M.; Buckle, A.M.; Moseley, G.W.; et al. Recognition by host nuclear transport proteins drives disorder-to-order transition in Hendra virus V. *Sci Rep* **2018**, *8*, 358, doi:10.1038/s41598-017-18742-8.
105. Oglesbee, M.; Ringler, S.; Krakowka, S. Interaction of canine distemper virus nucleocapsid variants with 70K heat-shock proteins. *J. Gen. Virol.* **1990**, *71*, 1585-1590.
106. Bhella, D.; Ralph, A.; Murphy, L.B.; Yeo, R.P. Significant differences in nucleocapsid morphology within the Paramyxoviridae. *J. Gen. Virol.* **2002**, *83*, 1831-1839.
107. Bhella, D.; Ralph, A.; Yeo, R.P. Conformational flexibility in recombinant measles virus nucleocapsids visualised by cryo-negative stain electron microscopy and real-space helical reconstruction. *J. Mol. Biol.* **2004**, *340*, 319-331.
108. Bhella, D. Measles virus nucleocapsid structure, conformational flexibility and the rule of six. In *Measles virus nucleoprotein*, Longhi, S., Ed.; Nova Publishers Inc.: Hauppauge, NY, 2007.
109. Tapparel, C.; Maurice, D.; Roux, L. The activity of Sendai virus genomic and antigenomic promoters requires a second element past the leader template regions: a motif (GNNNNN)<sub>3</sub> is essential for replication. *J. Virol.* **1998**, *72*, 3117-3128.
110. Dunker, A.K.; Garner, E.; Guillot, S.; Romero, P.; Albrecht, K.; Hart, J.; Obradovic, Z.; Kissinger, C.; Villafranca, J.E. Protein disorder and the evolution of molecular recognition: theory, predictions and observations. *Pac. Symp. Biocomput.* **1998**, *3*, 473-484.
111. Wright, P.E.; Dyson, H.J. Intrinsically unstructured proteins: re-assessing the protein structure-function paradigm. *J. Mol. Biol.* **1999**, *293*, 321-331., doi:10.1006/jmbi.1999.3110.
112. Dunker, A.K.; Obradovic, Z. The protein trinity--linking function and disorder. *Nat. Biotechnol.* **2001**, *19*, 805-806.
113. Dunker, A.K.; Lawson, J.D.; Brown, C.J.; Williams, R.M.; Romero, P.; Oh, J.S.; Oldfield, C.J.; Campen, A.M.; Ratliff, C.M.; Hipps, K.W.; et al. Intrinsically disordered protein. *J. Mol. Graph. Model.* **2001**, *19*, 26-59.
114. Dunker, A.K.; Brown, C.J.; Obradovic, Z. Identification and functions of usefully disordered proteins. *Adv Protein Chem* **2002**, *62*, 25-49.
115. Uversky, V.N.; Li, J.; Souillac, P.; Jakes, R.; Goedert, M.; Fink, A.L. Biophysical properties of the synucleins and their propensities to fibrillate: inhibition of alpha-synuclein assembly by beta- and gamma- synucleins. *J. Biol. Chem.* **2002**, *277*, 25.
116. Gunasekaran, K.; Tsai, C.J.; Kumar, S.; Zanuy, D.; Nussinov, R. Extended disordered proteins: targeting function with less scaffold. *Trends Biochem. Sci.* **2003**, *28*, 81-85.
117. Fink, A.L. Natively unfolded proteins. *Curr. Opin. Struct. Biol.* **2005**, *15*, 35-41.
118. Dyson, H.J.; Wright, P.E. Intrinsically unstructured proteins and their functions. *Nat. Rev. Mol. Cell Biol.* **2005**, *6*, 197-208.

119. Pancsa, R.; Fuxreiter, M. Interactions via intrinsically disordered regions: what kind of motifs? *IUBMB Life* **2012**, *64*, 513-520, doi:10.1002/iub.1034.
120. Uversky, V.N.; Kuznetsova, I.M.; Turoverov, K.K.; Zaslavsky, B. Intrinsically disordered proteins as crucial constituents of cellular aqueous two phase systems and coacervates. *FEBS Lett.* **2015**, *589*, 15-22, doi:10.1016/j.febslet.2014.11.028.
121. Wang, J.; Choi, J.M.; Holehouse, A.S.; Lee, H.O.; Zhang, X.; Jahnel, M.; Maharana, S.; Lemaitre, R.; Pozniakovsky, A.; Drechsel, D.; et al. A Molecular Grammar Governing the Driving Forces for Phase Separation of Prion-like RNA Binding Proteins. *Cell* **2018**, *174*, 688-699.e616, doi:10.1016/j.cell.2018.06.006.
122. Brocca, S.; Grandori, R.; Longhi, S.; Uversky, V. Liquid-Liquid Phase Separation by Intrinsically Disordered Protein Regions of Viruses: Roles in Viral Life Cycle and Control of Virus-Host Interactions. *Int J Mol Sci* **2020**, *21*, doi:10.3390/ijms21239045.
123. Etibor, T.A.; Yamauchi, Y.; Amorim, M.J. Liquid Biomolecular Condensates and Viral Lifecycles: Review and Perspectives. *Viruses* **2021**, *13*, doi:10.3390/v13030366.
124. Lopez, N.; Camporeale, G.; Salgueiro, M.; Borkosky, S.S.; Visentín, A.; Peralta-Martinez, R.; Loureiro, M.E.; de Prat-Gay, G. Deconstructing virus condensation. *PLoS Pathog* **2021**, *17*, e1009926, doi:10.1371/journal.ppat.1009926.
125. Pesce, G.; Brocca, S.; Grandori, R.; Longhi, S.; Uversky, A.V. Droplets of life: role of phase separation in virus replication and compartmentalization. In *Droplets of life*, Uversky, A.V., Ed.; Elsevier: 2022; Volume in press.
126. Wu, C.; Holehouse, A.S.; Leung, D.W.; Amarasinghe, G.K.; Dutch, R.E. Liquid Phase Partitioning in Virus Replication: Observations and Opportunities. *Annu Rev Virol* **2022**, doi:10.1146/annurev-virology-093020-013659.
127. Papa, G.; Borodavka, A.; Desselberger, U. Viroplasm: Assembly and Functions of Rotavirus Replication Factories. *Viruses* **2021**, *13*, doi:10.3390/v13071349.
128. Nevers, Q.; Albertini, A.A.; Lagaudrière-Gesbert, C.; Gaudin, Y. Negri bodies and other virus membrane-less replication compartments. *Biochim Biophys Acta Mol Cell Res* **2020**, *1867*, 118831, doi:10.1016/j.bbamcr.2020.118831.
129. Su, J.M.; Wilson, M.Z.; Samuel, C.E.; Ma, D. Formation and Function of Liquid-Like Viral Factories in Negative-Sense Single-Stranded RNA Virus Infections. *Viruses* **2021**, *13*, doi:10.3390/v13010126.
130. Zhou, Y.; Su, J.M.; Samuel, C.E.; Ma, D. Measles Virus Forms Inclusion Bodies with Properties of Liquid Organelles. *J. Virol.* **2019**, *93*, e00948-00919, doi:10.1128/JVI.00948-19.
131. Guseva, S.; Milles, S.; Jensen, M.R.; Schoehn, G.; Ruigrok, R.W.; Blackledge, M. Structure, dynamics and phase separation of measles virus RNA replication machinery. *Curr Opin Virol* **2020**, *41*, 59-67, doi:10.1016/j.coviro.2020.05.006.
132. Guseva, S.; Milles, S.; Ringkjøbing Jensen, M.; Salvi, N.; Kleman, J.; Maurin, D.; Ruigrok, R.W.; Blackledge, M. Measles virus nucleo- and phosphoproteins form liquid-like phase-separated compartments that promote nucleocapsid assembly. *Sci Adv* **2020**, *6*, eaaz7095, doi:10.1126/sciadv.aaz7095
133. Ringel, M.; Heiner, A.; Behner, L.; Halwe, S.; Sauerhering, L.; Becker, N.; Dietzel, E.; Sawatsky, B.; Kolesnikova, L.; Maisner, A. Nipah virus induces two inclusion body populations: Identification of novel inclusions at the plasma membrane. *PLoS Pathog* **2019**, *15*, e1007733, doi:10.1371/journal.ppat.1007733.
134. Boggs, K.B.; Cifuentes-Munoz, N.; Edmonds, K.; Najjar, F.E.; Ossandón, C.; Roe, M.; Moncman, C.L.; Creamer, T.; Dutch, R.E. Human metapneumovirus P protein independently drives phase separation and recruits N protein to liquid-like inclusion bodies. *bioRxiv* **2021**, 2021.2009.2024.461765, doi:10.1101/2021.09.24.461765.
135. Léger, P.; Nachman, E.; Richter, K.; Tamietti, C.; Koch, J.; Burk, R.; Kummer, S.; Xin, Q.; Stanifer, M.; Bouloy, M.; et al. NSs amyloid formation is associated with the virulence of Rift Valley fever virus in mice. *Nat Commun* **2020**, *11*, 3281, doi:10.1038/s41467-020-17101-y.

136. Dunker, A.K.; Cortese, M.S.; Romero, P.; Iakoucheva, L.M.; Uversky, V.N. Flexible nets. *FEBS J.* **2005**, *272*, 5129-5148.
137. Uversky, V.N.; Oldfield, C.J.; Dunker, A.K. Showing your ID: intrinsic disorder as an ID for recognition, regulation and cell signaling. *J Mol Recognit* **2005**, *18*, 343-384.
138. Haynes, C.; Oldfield, C.J.; Ji, F.; Klitgord, N.; Cusick, M.E.; Radivojac, P.; Uversky, V.N.; Vidal, M.; Iakoucheva, L.M. Intrinsic disorder is a common feature of hub proteins from four eukaryotic interactomes. *PLoS Comput Biol* **2006**, *2*, e100.
139. Bourhis, J.M.; Receveur-Bréchet, V.; Oglesbee, M.; Zhang, X.; Buccellato, M.; Darbon, H.; Canard, B.; Finet, S.; Longhi, S. The intrinsically disordered C-terminal domain of the measles virus nucleoprotein interacts with the C-terminal domain of the phosphoprotein via two distinct sites and remains predominantly unfolded. *Protein Sci.* **2005**, *14*, 1975-1992.
140. Iwasaki, M.; Takeda, M.; Shirogane, Y.; Nakatsu, Y.; Nakamura, T.; Yanagi, Y. The matrix protein of measles virus regulates viral RNA synthesis and assembly by interacting with the nucleocapsid protein. *J. Virol.* **2009**, *83*, 10374-10383, doi:10.1128/JVI.01056-09.
141. Zhang, X.; Glendering, C.; Linke, H.; Parks, C.L.; Brooks, C.; Udem, S.A.; Oglesbee, M. Identification and characterization of a regulatory domain on the carboxyl terminus of the measles virus nucleocapsid protein. *J. Virol.* **2002**, *76*, 8737-8746.
142. Zhang, X.; Bourhis, J.M.; Longhi, S.; Carsillo, T.; Buccellato, M.; Morin, B.; Canard, B.; Oglesbee, M. Hsp72 recognizes a P binding motif in the measles virus N protein C-terminus. *Virology* **2005**, *337*, 162-174.
143. Couturier, M.; Buccellato, M.; Costanzo, S.; Bourhis, J.M.; Shu, Y.; Nicaise, M.; Desmadril, M.; Flaudrops, C.; Longhi, S.; Oglesbee, M. High Affinity Binding between Hsp70 and the C-Terminal Domain of the Measles Virus Nucleoprotein Requires an Hsp40 Co-Chaperone. *J Mol Recognit* **2010**, *23*, 301-315.
144. Sato, H.; Masuda, M.; Miura, R.; Yoneda, M.; Kai, C. Morbillivirus nucleoprotein possesses a novel nuclear localization signal and a CRM1-independent nuclear export signal. *Virology* **2006**, *352*, 121-130.
145. tenOever, B.R.; Servant, M.J.; Grandvaux, N.; Lin, R.; Hiscott, J. Recognition of the Measles Virus Nucleocapsid as a Mechanism of IRF-3 Activation. *J. Virol.* **2002**, *76*, 3659-3669.
146. Colombo, M.; Bourhis, J.M.; Chamontin, C.; Soriano, C.; Villet, S.; Costanzo, S.; Couturier, M.; Belle, V.; Fournel, A.; Darbon, H.; et al. The interaction between the measles virus nucleoprotein and the Interferon Regulator Factor 3 relies on a specific cellular environment. *Virol J* **2009**, *6*, 59, doi:10.1186/1743-422X-6-59.
147. Laine, D.; Bourhis, J.; Longhi, S.; Flacher, M.; Cassard, L.; Canard, B.; Sautès-Fridman, C.; Roubourdin-Combe, C.; Valentin, H. Measles virus nucleoprotein induces cell proliferation arrest and apoptosis through NTAIL/NR and N CORE/FcgRIIB1 interactions, respectively. *J. Gen. Virol.* **2005**, *86*, 1771-1784.
148. Laine, D.; Trescol-Biémont, M.; Longhi, S.; Libeau, G.; Marie, J.; Vidalain, P.; Azocar, O.; Diallo, A.; Canard, B.; Roubourdin-Combe, C.; et al. Measles virus nucleoprotein binds to a novel cell surface receptor distinct from FcgRII via its C-terminal domain: role in MV-induced immunosuppression. *J. Virol.* **2003**, *77*, 11332-11346.
149. Watanabe, A.; Yoneda, M.; Ikeda, F.; Sugai, A.; Sato, H.; Kai, C. Peroxiredoxin 1 is required for efficient transcription and replication of measles virus. *J. Virol.* **2011**, *85*, 2247-2253, doi:10.1128/JVI.01796-10.
150. De, B.P.; Banerjee, A.K. Involvement of actin microfilaments in the transcription/replication of human parainfluenza virus type 3: possible role of actin in other viruses. *Microsc. Res. Tech.* **1999**, *47*, 114-123.
151. Moyer, S.A.; Baker, S.C.; Horikami, S.M. Host cell proteins required for measles virus reproduction. *J. Gen. Virol.* **1990**, *71*, 775-783.
152. Orchard, S.; Ammari, M.; Aranda, B.; Breuza, L.; Briganti, L.; Broackes-Carter, F.; Campbell, N.H.; Chavali, G.; Chen, C.; del-Toro, N.; et al. The MIntAct project--IntAct as a common

- curation platform for 11 molecular interaction databases. *Nucleic Acids Res.* **2014**, *42*, D358-363, doi:10.1093/nar/gkt1115.
153. Chen, M.; Cortay, J.C.; Gerlier, D. Measles virus protein interactions in yeast: new findings and caveats. *Virus Res.* **2003**, *98*, 123-129, doi: **10.1016/j.virusres.2003.09.003**.
  154. Devaux, P.; Priniski, L.; Cattaneo, R. The measles virus phosphoprotein interacts with the linker domain of STAT1. *Virology* **2013**, *444*, 250-256, doi:10.1016/j.virol.2013.06.019.
  155. Ker, D.; Jenkins, H.; Greive, S.; Antson, A. CryoEM structure of the Nipah virus nucleocapsid assembly. *BioRxiv* **2020**, doi:doi.org/10.1101/2020.01.20.912261
  156. Yabukarski, F.; Leyrat, C.; Martinez, N.; Communie, G.; Ivanov, I.; Ribeiro, E.A., Jr.; Buisson, M.; Gerard, F.C.; Bourhis, J.M.; Jensen, M.R.; et al. Ensemble Structure of the Highly Flexible Complex Formed between Vesicular Stomatitis Virus Unassembled Nucleoprotein and its Phosphoprotein Chaperone. *J. Mol. Biol.* **2016**, *428*, 2671-2694, doi:10.1016/j.jmb.2016.04.010.
  157. Jamin, M.; Yabukarski, F. Nonsegmented Negative-Sense RNA Viruses-Structural Data Bring New Insights Into Nucleocapsid Assembly. *Adv. Virus Res.* **2017**, *97*, 143-185, doi:10.1016/bs.aivir.2016.09.001.
  158. Jordan, I.K.; Sutter, B.A.; McClure, M.A. Molecular evolution of the Paramyxoviridae and Rhabdoviridae multiple-protein-encoding P gene. *Mol. Biol. Evol.* **2000**, *17*, 75-86, doi: 10.1093/oxfordjournals.molbev.a026240
  159. Narechania, A.; Terai, M.; Burk, R.D. Overlapping reading frames in closely related human papillomaviruses result in modular rates of selection within E2. *J. Gen. Virol.* **2005**, *86*, 1307-1313, doi:10.1099/vir.0.80747-0.
  160. Rancurel, C.; Khosravi, M.; Dunker, K.A.; Romero, P.R.; Karlin, D. Overlapping genes produce proteins with unusual sequence properties and offer insight into de novo protein creation. *J. Virol.* **2009**, *83*, 10719-10736, doi:10.1128/JVI.00595-09.
  161. Kovacs, E.; Tompa, P.; Liliom, K.; Kalmar, L. Dual coding in alternative reading frames correlates with intrinsic protein disorder. *Proc Natl Acad Sci U S A* **2010**, *107*, 5429-5434, doi:10.1073/pnas.0907841107.
  162. Karlin, D.; Longhi, S.; Receveur, V.; Canard, B. The N-terminal domain of the phosphoprotein of morbilliviruses belongs to the natively unfolded class of proteins. *Virology* **2002**, *296*, 251-262.
  163. Bourhis, J.M.; Canard, B.; Longhi, S. Structural disorder within the replicative complex of measles virus: functional implications. *Virology* **2006**, *344*, 94-110, doi:10.1016/j.virol.2005.09.025.
  164. Kumar, N.; Kaushik, R.; Tennakoon, C.; Uversky, V.N.; Longhi, S.; Zhang, K.Y.J.; Bhatia, S. Comprehensive Intrinsic Disorder Analysis of 6108 Viral Proteomes: From the Extent of Intrinsic Disorder Penetration to Functional Annotation of Disordered Viral Proteins. *J Proteome Res* **2021**, doi:10.1021/acs.jproteome.1c00011.
  165. Xue, B.; Blocquel, D.; Habchi, J.; Uversky, A.V.; Kurgan, L.; Uversky, V.N.; Longhi, S. Structural disorder in viral proteins. *Chem Rev* **2014**, *114*, 6880-6911, doi:10.1021/cr4005692.
  166. Davey, N.E.; Trave, G.; Gibson, T.J. How viruses hijack cell regulation. *Trends Biochem. Sci.* **2011**, *36*, 159-169, doi:10.1016/j.tibs.2010.10.002.
  167. Tokuriki, N.; Oldfield, C.J.; Uversky, V.N.; Berezovsky, I.N.; Tawfik, D.S. Do viral proteins possess unique biophysical features? *Trends Biochem. Sci.* **2009**, *34*, 53-59, doi:10.1016/j.tibs.2008.10.009.
  168. Xue, B.; Williams, R.W.; Oldfield, C.J.; Goh, G.K.; Dunker, A.K.; Uversky, V.N. Viral disorder or disordered viruses: do viral proteins possess unique features? *Protein Pept Lett* **2010**, *17*, 932-951, doi:10.2174/092986610791498984.
  169. Vavouri, T.; Semple, J.I.; Garcia-Verdugo, R.; Lehner, B. Intrinsic protein disorder and interaction promiscuity are widely associated with dosage sensitivity. *Cell* **2009**, *138*, 198-208, doi:10.1016/j.cell.2009.04.029.
  170. Babu, M.M.; van der Lee, R.; de Groot, N.S.; Gsponer, J. Intrinsically disordered proteins: regulation and disease. *Curr. Opin. Struct. Biol.* **2011**, *21*, 432-440, doi:10.1016/j.sbi.2011.03.011.

171. Gsponer, J.; Futschik, M.E.; Teichmann, S.A.; Babu, M.M. Tight regulation of unstructured proteins: from transcript synthesis to protein degradation. *Science* **2008**, *322*, 1365-1368, doi:10.1126/science.1163581.
172. Betzi, S.; Restouin, A.; Opi, S.; Arold, S.T.; Parrot, I.; Guerlesquin, F.; Morelli, X.; Collette, Y. Protein protein interaction inhibition (2P2I) combining high throughput and virtual screening: Application to the HIV-1 Nef protein. *Proc Natl Acad Sci U S A* **2007**, *104*, 19256-19261.
173. Cheng, Y.; Legall, T.; Oldfield, C.J.; Mueller, J.P.; Van, Y.Y.; Romero, P.; Cortese, M.S.; Uversky, V.N.; Dunker, A.K. Rational drug design via intrinsically disordered protein. *Trends Biotechnol.* **2006**, *24*, 435-442.
174. Uversky, V.N. Targeting intrinsically disordered proteins in neurodegenerative and protein dysfunction diseases: another illustration of the D(2) concept. *Expert Rev Proteomics* **2010**, *7*, 543-564, doi:10.1586/epr.10.36.
175. Dunker, A.K.; Uversky, V.N. Drugs for 'protein clouds': targeting intrinsically disordered transcription factors. *Curr Opin Pharmacol* **2010**, *10*, 782-788, doi:10.1016/j.coph.2010.09.005.
176. Uversky, V.N. Intrinsic disorder-based protein interactions and their modulators. *Curr. Pharm. Des.* **2012**, *19*, 4191-213, doi: 10.2174/1381612811319230005.
177. Uversky, V.N. Intrinsically disordered proteins and novel strategies for drug discovery. *Expert Opin Drug Discov.* **2012**, *7*, 475-488, doi: 10.1517/17460441.2012.686489.
178. Marasco, D.; Scognamiglio, P.L. Identification of Inhibitors of Biological Interactions Involving Intrinsically Disordered Proteins. *Int J Mol Sci* **2015**, *16*, 7394-7412, doi:10.3390/ijms16047394.
179. Joshi, P.; Vendruscolo, M. Druggability of Intrinsically Disordered Proteins. *Adv. Exp. Med. Biol.* **2015**, *870*, 383-400, doi:10.1007/978-3-319-20164-1\_13.
180. Galloux, M.; Gabiane, G.; Sourimant, J.; Richard, C.A.; England, P.; Moudjou, M.; Aumont-Nicaise, M.; Fix, J.; Rameix-Welti, M.A.; Eleouet, J.F. Identification and characterization of the binding site of the respiratory syncytial virus phosphoprotein to RNA-free nucleoprotein. *J. Virol.* **2015**, doi:10.1128/JVI.03666-14.
181. Communie, G.; Habchi, J.; Yabukarski, F.; Blocquel, D.; Schneider, R.; Tarbouriech, N.; Papageorgiou, N.; Ruigrok, R.W.; Jamin, M.; Jensen, M.R.; et al. Atomic resolution description of the interaction between the nucleoprotein and phosphoprotein of Hendra virus. *PLoS Pathog* **2013**, *9*, e1003631, doi:10.1371/journal.ppat.1003631.
182. Bourgeas, R.; Basse, M.J.; Morelli, X.; Roche, P. Atomic analysis of protein-protein interfaces with known inhibitors: the 2P2I database. *PLoS ONE* **2010**, *5*, e9598, doi:10.1371/journal.pone.0009598.
183. Wang, S.; Dai, T.; Qin, Z.; Pan, T.; Chu, F.; Lou, L.; Zhang, L.; Yang, B.; Huang, H.; Lu, H.; et al. Targeting liquid-liquid phase separation of SARS-CoV-2 nucleocapsid protein promotes innate antiviral immunity by elevating MAVS activity. *Nat. Cell Biol.* **2021**, *23*, 718-732, doi:10.1038/s41556-021-00710-0.
184. Risso-Ballester, J.; Galloux, M.; Cao, J.; Le Goffic, R.; Hontonnou, F.; Jobart-Malfait, A.; Desquesnes, A.; Sake, S.M.; Haid, S.; Du, M.; et al. A condensate-hardening drug blocks RSV replication in vivo. *Nature* **2021**, *595*, 596-599, doi:10.1038/s41586-021-03703-z.